GEOLOGIAN TUTKIMUSKESKUS — GEOLOGISKA FORSKNINGSCENTRALEN
GEOLOGICAL SURVEY OF FINLAND

Opas — Guide 33

IGCP Project 315

FINLAND 1991

Correlation of Rapakivi Granites and Related Rocks on a Global Scale

**Symposium**

**RAPAKIVI GRANITES AND RELATED ROCKS**

July 29—31, 1991, University of Helsinki, Finland

Excursion

# SALMI BATHOLITH AND PITKÄRANTA ORE FIELD IN SOVIET KARELIA

August 1—4, 1991

**With contributions by**

**Yu. Amelin, A. Beljaev, A. Larin, L. Neymark, and K. Stepanov**

**Edited by**

**Ilmari Haapala, O. Tapani Rämö, and Pekka T. Salonsaari**

Espoo 1991

Cover: Wiborgite

GEOLOGIAN TUTKIMUSKESKUS - GEOLOGISKA FORSKNINGSCENTRALEN

GEOLOGICAL SURVEY OF FINLAND

Opas - Guide 33

IGCP Project 315

Correlation of Rapakivi Granites and Related Rocks on a Global Scale


Symposium

**RAPAKIVI GRANITES AND RELATED ROCKS**

July 29-31, 1991, University of Helsinki, Finland

**EXCURSION**

# SALMI BATHOLITH AND PITKÄRANTA ORE FIELD IN SOVIET KARELIA

August 1-4, 1991

With contributions by

Yu. Amelin, A. Beljaev, A. Larin, L. Neymark, and K. Stepanov

Edited by

Ilmari Haapala, O. Tapani Rämö, and Pekka T. Salonsaari

Espoo 1991

ISBN 951-690-436-X
ISSN 0781-643X

## PREFACE

The IGCP project 315 (Rapakivi granites and related rocks) is arranging the first symposium and inaugural meeting on July 29-31, 1991, in the University of Helsinki, Finland. The symposium is followed on August 1-4 by a field trip to the Vyborg (Wiborg) rapakivi area in southeastern Finland as well as to the Salmi rapakivi area in Karelia, USSR.

This excursion guide deals with the geological background and modern achievements in petrology and ore geology of the Salmi batholith and the Pitkäranta ore field. Regarding the Finnish part of the field trip, there are recently written papers and field trip guides, and some of these will be handed out to the excursion participants.

The manuscript of this guide was originally written in Russian; Mr. Boris Saltikoff of the Geological Survey of Finland translated it into English. After editorial changes and corrections, the English was checked by Mr. Donald Smart of the University of Helsinki. Professor Kauko Korpela, acting Director of the Geological Survey of Finland, gave permission to publish the guide in the series of the Geological Survey. The editors wish to express their sincere thanks to the named persons and to the authors for a good cooperation.

Rapakivi granites are important and fascinating rocks and constitute an essential part of many Precambrian shield areas. Their significance to the evolution of the Proterozoic continental crust and to economic geology (building stones, tin and related deposits) should not be underestimated.

Looking forward to a successful field trip,

Ilmari Haapala O. Tapani Rämö Pekka T. Salonsaari

# CONTENTS

## INTRODUCTION

Anorthosite and rapakivi granite intrusions are widespread on a global scale, typically comprising elongated non-continuous belts in Precambrian shield areas. This magmatic association was formed between 1.75 and 1.0 Ga. Emplacement of the plutons of the anorthosite-rapakivi assemblage is attributed by most authors to incipient rifting (e.g., Emslie, 1985; Anderson, 1983; Windley, 1983; Nurmi & Haapala, 1986). Anderson (1983) relates these rocks to incipient rift evolution interrupted in an early pre-rift stage, while Windley (1983) classifies the intrusion belts as "abortive rift structures". Temporally associated with the anorthosite-rapakivi plutons are bimodal volcanites, with a predominance of acidic volcanics as well as quartz porphyry and dolerite dykes.

Rapakivi granites are accompanied by tin, rare metal, and polymetal ore mineralization, in some cases on an industrial scale. The largest tin deposit related to rapakivi granites is the Pitinga Mine in Brazil (Daoud & Fuck, 1989).

Within the East European platform the plutons of the anorthosite - rapakivi assemblage constitute a huge northwest-trending non-continuous belt that follows the western margin of the platform. This belt extends for more than 2000 km from Ukraine through Belorussia, Poland, and the Baltic region to Fennoscandia (Fig. 1). Another ca. 1000 km long east-west-trending belt can be traced along the southern margin of the Baltic (Fennoscandian) shield. The two belts join in southern Fennoscandia (Fig. 1). The age of the intrusions ranges from 1.77 to 1.54 Ga. The oldest intrusions (Korosten and Mirgorod batholiths) are found in the southern part of the former belt in the Ukrainian shield and show a U-Pb zircon ages from 1.77 to 1.75 Ga (Scherbak et al., 1989). Intrusions of two age groups are distributed in the Fennoscandian shield, these are: the Wiborg batholith with U-Pb zircon ages of 1.65 to 1.63 Ga and the batholiths of Laitila, Vehmaa, Åland, and Salmi with U-Pb zircon ages of 1.59 to 1.54 Ga (Vaasjoki, 1977; Vaasjoki et al., 1991; Shergina et al., 1982).

In several cases younger depressions (grabens), filled with Jotnian terrigenous and volcanic-terrigenous rocks are associated with anorthosite and rapakivi granite plutons. The volcanic rocks are tholeiitic lavas and tuffs. The age of Jotnian sedimentary rocks has been determined to be 1.3 to 1.4 Ga (Rb-Sr and K-Ar ages; cf. Simonen, 1980). The Jotnian troughs are also intruded by dyke swarms, sills, and minor stratified intrusions of gabbro-doleritic to monzonitic composition. Emplacement of these rocks took place in two magmatic pulses dated at 1.35 to 1.37 and 1.22 to 1.27 Ga (Welin & Lundqvist, 1975; Patchett, 1978). According to Haapala and Rämö (1990) the Jotnian structures represent a later rifting event within the anorthosite - rapakivi granite belt.

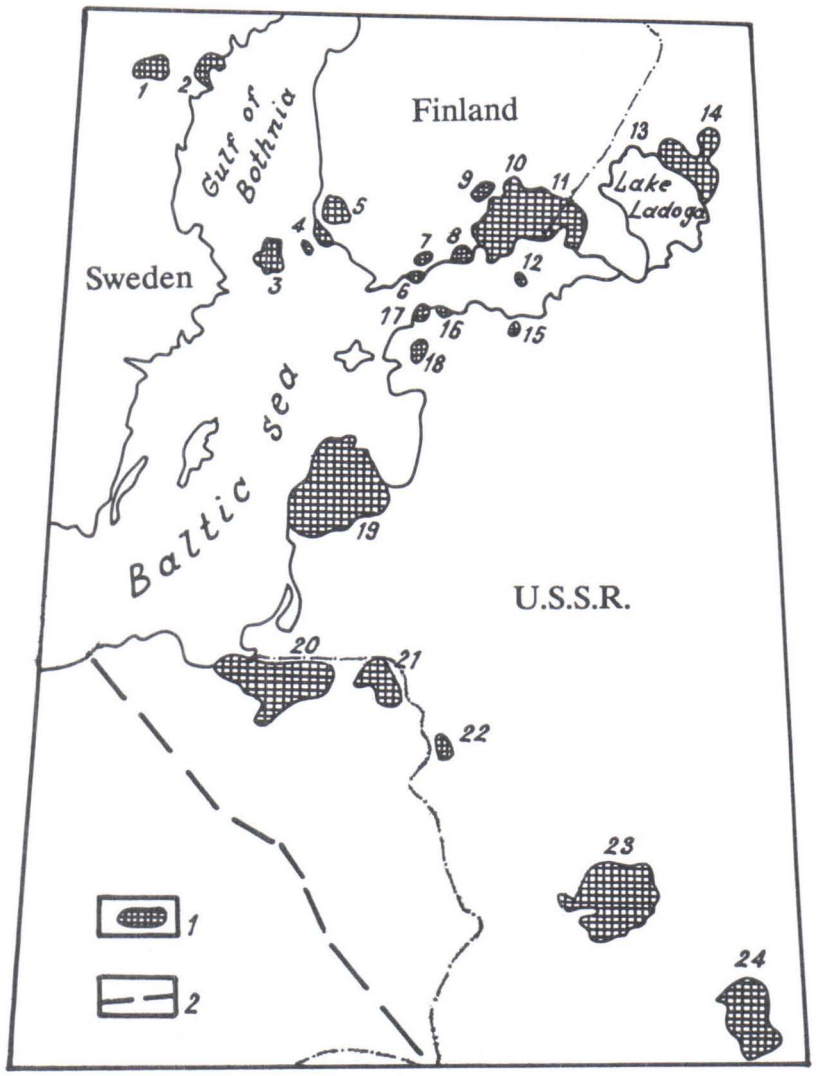


Fig. 1. Plutons of the anorthosite - rapakivi granite assemblage in the Eastern European platform (modified after Velikoslavinskiy et al., 1978). **1**: anorthosite - rapakivi granite plutons (1 - Ragunda, 2 - Nordingrå, 3 - Åland, 4 - Vehmaa, 5 - Laitila, 6 - Obbnäs, 7 - Bodom, 8 - Onas, 9 - Ahvenisto, 10 - Suomenniemi, 11 - Wiborg, 12 - Hogland (Suursaari), 13 - Salmi, 14 - Ulalega, 15 - Ereda, 16 - Neeme, 17 - Naissaari, 18 - Marjamaa, 19 - Riga, 20-21 - Polish-Mazurian complex, 22 - Belorussian, 23 - Korosten, 24 - Korsun-Novomirgorod); **2**: western margin of the East European platform.

## 1. GEOLOGICAL SETTING OF THE SALMI BATHOLITH

The Salmi batholith is situated at the eastern edge of the east-west-trending anorthosite - rapakivi granite belt in the southern Fennoscandian shield (Fig. 1). The Salmi batholith follows the margin of the Svecokarelian fold belt and Karelian craton. The emplacement of the batholith took place along an upthrust zone between these two large units (Fig. 2). The rocks of the batholith cut late Archean granitoids and

supracrustal rocks in greenstone belts belonging to the Karelian craton, as well as the lower Proterozoic metamorphic formations of the Jatulian terrigenous - carbonatic unit and the Svecokarelian gneiss - schist unit (granite gneiss in the domes, marble and amphibole schist of the Pitkäranta suite which frames these domes, and the flysch strata of the Ladoga series). The southwestern part of the batholith its overlain by terrigenous - volcanic Jotnian strata (the Salmi suite) and is intersected by dykes and minor layered intrusions that are comagmatic with the volcanics of the Salmi suite.

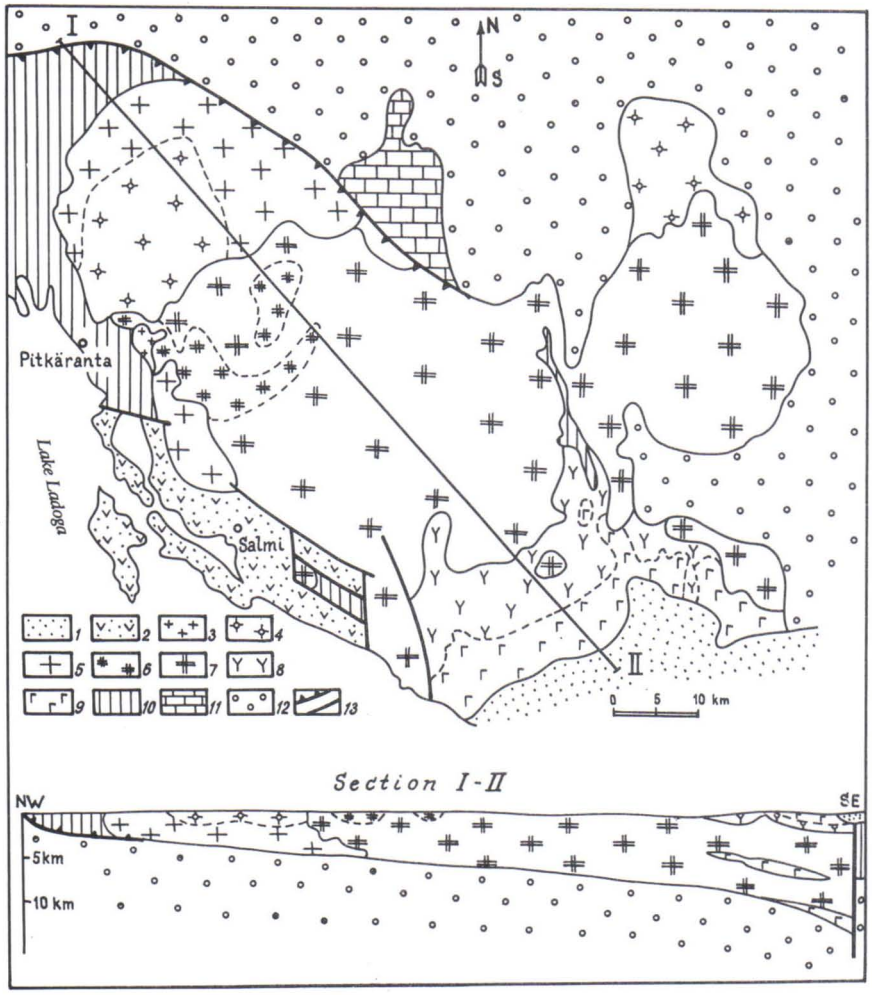


Fig. 2. Geological structure of the Salmi anorthosite - rapakivi granite batholith. **1**: sedimentary rocks of the East European platform; **2**: volcanogenic - terrigenous Jotnian rocks (Salmi suite); **3-9**: magmatic rocks of the Salmi batholith: 3 - albite-protolithionite granite, 4 - porphyritic biotite granite with a fine-grained groundmass, 5 - even-grained biotite granite, 6 - porphyritic biotite-amphibole granite with a fine-grained groundmass, 7 - coarse-grained biotite-amphibole granites (wiborgite and pyterlite), 8 - monzonite and quartz syenite, 9 - gabbronorite, gabbro, anorthosite; **10**: Svecokarelian gneiss - schist complex; **11**: Jatulian terrigenous and carbonate complex; **12**: Lopian granite - greenschist complex; **13** - thrusts and fractures.

## 2. INTERNAL STRUCTURE AND COMPOSITION OF THE SALMI BATHOLITH

There are five main rock groups in the Salmi batholith: gabbros, gabbronorites, and anorthosites; monzonites and quartz syenites; amphibole-biotite granites; biotite granites; and albite-protolithionite granites (Sviridenko, 1968; Velikoslavinskiy et al., 1978; Shinkarev et al., 1973; Bantova et al., 1975). The batholith is asymmetrically zoned (Fig. 2). Moving from the southeast, where a root channel is expected to occur on the basis of geophysical data, to northwest, a regular compositional change is encountered. It is assumed that the rocks of the first four groups comprise sheet-like bodies plunging to the southeast.

### Basic rocks

Basic rocks are widespread in the buried southern part of the batholith and have been discovered by drilling (Shinkarev & Anischenkova, 1973; Bantova et al., 1975). According to Shustova (in Velikoslavinskiy et al., 1978) they follow zones of high gradients of the gravity field interpreted as deep fractures. Rock bodies of the gabbro-anorthosite complex are, however, poorly seen in geophysical maps, in spite of the fact that these rocks differ significantly from rapakivi granites in terms of their density and magnetic susceptibility. Geophysical data suggest that the basic rocks comprise relatively thin sheets and have granitic rocks beneath them.

The basic rocks include anorthosites, gabbro anorthosites, gabbros, and gabbronorites. Sometimes they show a vertical mutual transition in this order. The mineral composition of the rocks in the complex changes gradually from gabbronorites to anorthosites as follows: hypersthene (29 to 0 %), augite (9 to 30 %), fayalite (5 to 0 %), amphibole (1 to 0 %) and plagioclase $An_{54-42}$ (48 to 88 %). Accessory minerals include titanomagnetite, apatite and zircon; secondary minerals are a light green amphibole, biotite, and chlorite. Besides, potassium feldspar (orthoclase microperthite) is sometimes present in the gabbronorites and anorthosites occurring as veinlets and spots in plagioclase and in the mesostasis. Monzogabbros with 17 to 25 % potassium feldspar are also met with. The potassium feldspar has often a reaction relation with plagioclase; myrmekite texture is common at the boundaries between these minerals. Sometimes the myrmekites follow cracks which cross the plagioclase grains.

## Monzonites and quartz syenites

Monzonites and quartz syenites show a close association with anorthosites and gabbros. These can often be traced along the boundaries between rapakivi granites and gabbronorites.

The following minerals occur in monzonites and quartz syenites: hortonolite (0.9 to 0.8 %), hypersthene (8 to 0.5 %), augite (17 to 8 %), amphibole (1 to 4 %), biotite (1 to 2 %), plagioclase $An_{50-32}$ (49 to 31 %), orthoclase microperthite (3 to 31 %), and quartz (5 to 20 %). Myrmekite is found both in the monzonites and quartz syenites. Accessory minerals include titanomagnetite, apatite and zircon; secondary ones are light green amphibole, biotite, and chlorite.

Unfortunately, it is impossible to construct a clear picture of the interrelations between the gabbro-anorthosite, monzonites, syenites, and rapakivi granites using drilling data alone (Shinkarev & Anischenkova, 1973).

## Amphibole-biotite rapakivi granites

Granites of this group make up two-thirds of the exposed area of the batholith and comprise three varieties:

1. Coarse-grained amphibole-biotite granites. Both granites with oligoclase-mantled potassium feldspar ovoids (wiborgites) and varieties with scarce plagioclase rims and rounded potash feldspar ovoids (pyterlites) belong to this group. These granites comprise more than 90 % of amphibole-biotite granites.
2. Porphyritic amphibole-biotite granites with a fine-grained groundmass. This type is abundant mainly in the zone of the western endocontact, but also forms linear bodies maximum width of one km within the granites of the first variety.
3. Fine-grained aplitic granites. These occur as dykes following orthogonal cracks in the granites belonging to the two former varieties.

The contacts of the amphibole-biotite granites against the wall rocks are usually sharp and have 10 to 50 cm thick chilled margins. This zone consists of small-grained granite similar in composition with dyke granites.

The mineral composition of the amphibole-biotite granites shows a regular change from coarse-grained through porphyric to dyke varieties as follows (in percents): orthoclase-perthite (56-56-55), plagioclase $An_{18-28}$ (12-9-8.5), quartz (29-32-33), hastingsite (1.2-0.8-0.4); accessory minerals (in g/t): magnetite (5), hematite (330-110-120), ilmenite (1400-1100-400), anatase (10-5), orthite/bastnaesite (600-1000-1000),

zircon (900-660-250), apatite (130-80-15), fluorite (730-1000-600), molybdenite (20-10-10); and other components present in amounts less than 5 g/t: garnet, titanite, pyrite, spinel, sillimanite, tourmaline, and sometimes cassiterite.

### Biotite granites

Non-ovoidal biotite granites make up the northern and north - western parts of the batholith. As in the amphibole-biotite granites, three structural varieties can be distinguished:

1. Even-grained granites.
2. Porphyritic granites with a fine-grained groundmass. These constitute both linear bodies with distinct contacts within the even-grained granites and extensive rock masses with gradual transitions into granites of the first group.
3. Fine-grained dyke which fill cracks in granites of the two first varieties.

The biotite granites cut the biotite-amphibole granites. The mineral content of the biotite granites varies regularly from the even-grained varieties to porphyritic and to the fine-grained vein granites as follows (in percentages): orthoclase-perthite (52.5-52.0-51.0), plagioclase $An_{5-20}$ (10.5-10.5-8.5), quartz (34.5-34.5-38), biotite (2.8-2.9-2.2); accessory minerals (in g/t): magnetite (800-120-5), hematite (800-680-450), ilmenite (340-580-42), anatase (10-22-5), orthite/bastnaesite (700-250-150), zircon (460-340-150), apatite (5-5-5), fluorite (2200-2100-700) and molybdenite (12-5-5); and further, in amounts less than 5 g/t: garnet, titanite, pyrite, spinel, sillimanite, tourmaline, cassiterite and xenotime. Among the even-grained biotite granites there are dark-coloured greenish varieties with fayalite replacing magnetite. Slightly albitized and muscovitized varieties occur among the porphyritic biotite granites and cutting aplite dykes. They show slightly less orthoclase (up to 45 to 8 %), more quartz ( up to 36 to 37 %), and are characterized by the presence of albite and muscovite as well. The fluorite content increase to 2840 g/t, and tantalite-columbite and topaz are also present.

### Topaz-bearing albite-protolithionite granites

The granites of this group constitute several series of small dykes, stocks and minor dome-shaped intrusions within the amphibole-biotite granites, biotite granites, and metamorphic country rocks. Granites of this group have predominantly a fine-grained aplitic texture, while stocksheider-type pegmatites are often present along the borders

and in the apical parts of the dykes and dome structures. These contain skeletal quartz crystals, big crystals of microcline cutting the banding, as well as crystals of protolithionite and topaz (Fig. 3).

Fig. 3. Stockscheider (polished surface). Gently dipping dyke in the gneiss-granites of the Uuksu dome.

The aplitic granites of this group consist of microcline (15 %), plagioclase $An_{3-10}$ with several varieties of albite (45 %), quartz (35 %) and protolithionite* (5 %). The accessories are (in g/t) magnetite (5), hematite (120), ilmenite (40), anatase (5), orthite (5), zircon (40), apatite (5), fluorite (2700), molybdenite (5) and tantalite-columbite (55), as well as garnet, titanite, pyrite, spinel, kyanite, cassiterite, xenotime and topaz.

The granites of this group have sharp, occasionally brecciated, contacts with the surrounding rocks.

## 3. GEOCHEMISTRY

Geochemically, the Salmi batholith is made up of two series of magmatic rocks: a gabbronorite - anorthosite series and a monzonite - quartz syenite - rapakivi granite series.

* For definition, see Foster (1960).

In the rocks of the first series, the sequence from olivine-bearing gabbronorite to anorthosite shows a regular increase in the contents of $Al_2O_3$, CaO, and $Na_2O$, a slight increase in $K_2O$ and a decrease in FeO, MgO, and $TiO_2$ (Fig. 4). The regular trace elements variations (Fig. 5) and especially the REE-patterns (Fig. 6) suggest that the gabbronorites and anorthosites are differentiation of a single magma.

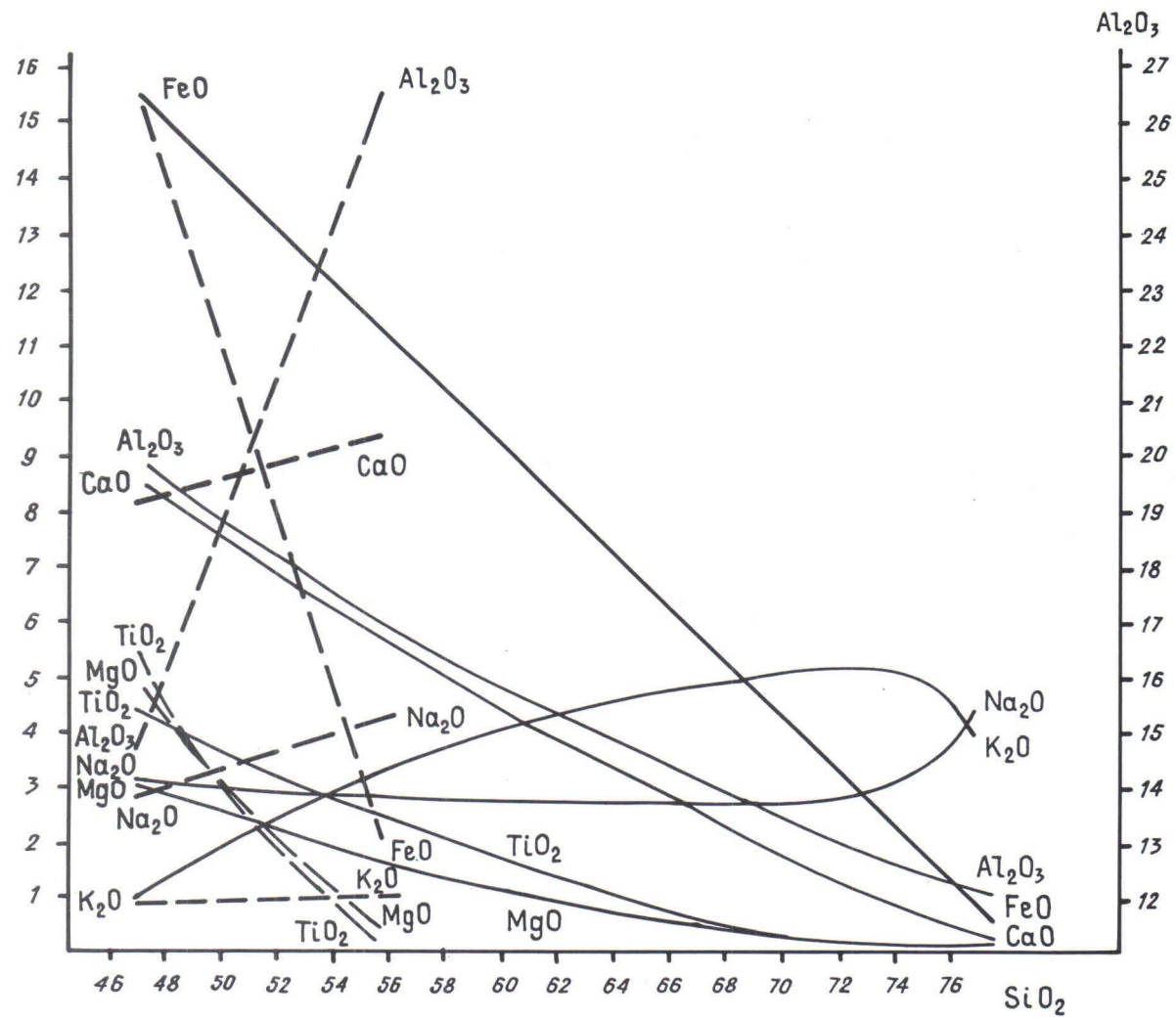


Fig. 4. Harker diagrams of the mean chemical compositions of the rocks of the Salmi batholith. Dashed lines: the gabbronorite - anorthosite series; solid lines: the monzonite - quartz syenite - amphibole-biotite granite - biotite granite - albite-protolithionite granite series. Vertical axis on the right: contents of $Al_2O_3$; vertical axis on the left: contents of other oxides (wt. %).

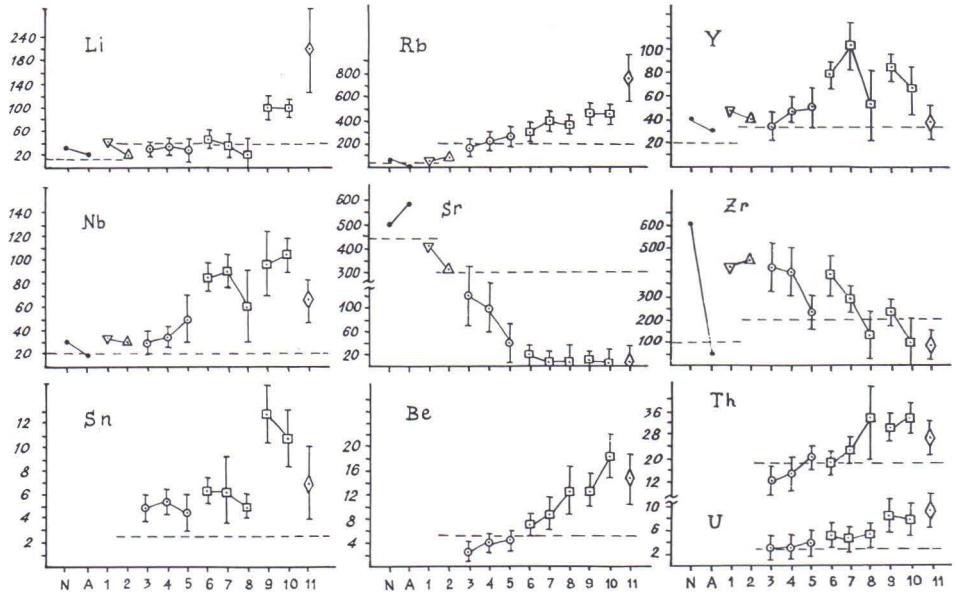


Fig. 5. Contents (in ppm) of the trace elements in the rocks of the Salmi batholith. **N**: gabbronorites; **A**: anorthosites; **1**: monzonites; **2**: quartz syenites; **3-5**: amphibole-biotite granites: 3 - coarse-grained (wiborgites and pyterlites), 4 - porphyritic with fine-grained groundmass, 5 - fine-grained vein granites; **6-10**: biotite granites: 6 - even-grained, 7 - porphyritic with fine-grained groundmass, 8 - fine-grained vein granites, 9-10 - like 7-8, but slightly albitized and muskovitized; **11**: fine-grained albite-protolithionite dyke granites. Horizontal dashed lines = Clarke values for elements for basic and acidic rocks according to Vinogradov (1962). Vertical segments around the dots = confidence ranges of the arithmetic mean for granites.

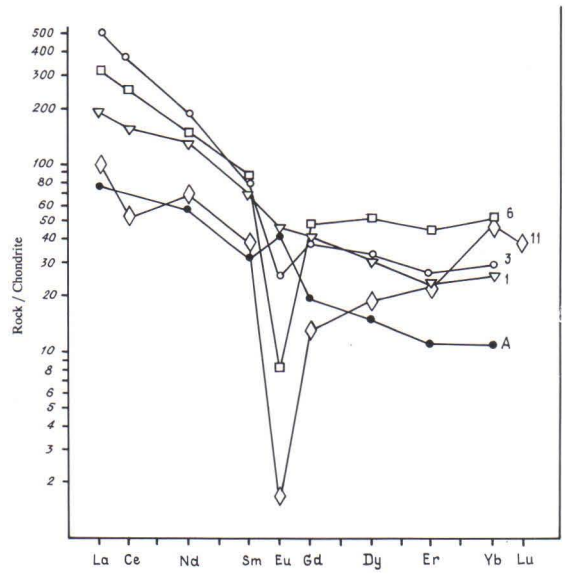


Fig. 6. Chondrite-normalized REE distribution in rocks of the Salmi batholith. **A**: anorthosite; **1**: monzonite gabbro; **3**: coarse-grained amphibole-biotite granite; **6**: even-grained biotite granite; **11**: albite-protolithionite granite.

A special feature of the basic rocks in the Salmi batholith are the very low contents of Cr, Ni, Co, V, Mn (A. Larin, unpublished data) and very high concentrations of REE as compared with basic rocks of the Proterozoic anorthosite complexes in general. Even among the anorthosite - rapakivi granite plutons of the East European platform, the basic rocks of the Salmi batholith are distinguished by their high REE concentrations.

The regression curves of the monzonite - quartz syenite - rapakivi granites magmatic series (Fig. 4) differ significantly from those of the basic rock series. From monzonites to granites there is a clear decrease in FeO, $Al_2O_3$, CaO, $TiO_2$ and MgO, an increase in $K_2O$ and very small changes in $Na_2O$. At the level of 73 % $SiO_2$ in granites the $K_2O$ content starts to decrease and $Na_2O$ content to increase. With increasing of $SiO_2$, Li, Rb, Nb, Sn, Be, U, and Th increase, and Ba, Sr and Zr decrease (Fig. 5), and a strengthening of the differentiation of granitoids (Fig. 9).

The regular variation of the REE contents in the gabbros, monzonites, and biotite-amphibole granites and biotite granites may be attributed to crystallization differentiation. Generally, LREE are strongly fractionated and enriched in the main phase of the rapakivi granites. The negative Eu anomaly is clearly visible. The distribution of REE in rapakivi granites of the main phase is very similar to that in the A-type granites. In late biotite granites, an inversion of REE takes place: the content of LREE decreases and that of HREE increases, together with an increase in the negative Eu anomaly. The distribution of REE during the differentiation processes is possibly caused by fractionation of feldspars (plagioclase may concentrate Eu), clinopyroxene, and hastingsite as well as accessory minerals like zircon and fluorite (concentrations of HREE) and orthite (a concentrator of LREE).

A different REE distribution is revealed by the albite-protolithionite granites (Fig. 6). They are very low in LREE (Ce is lower than the Clarke value for granites), and the negative Eu anomaly is extreme, but the content of Yb is practically unchanged as compared with the biotite granites. This distribution may be related to stabilization of halogene complexes in a fluid saturated melt (Kolker et al., 1990) or to metasomatic processes producing secondary fluorite with high concentrations of Yb. According to Beljaev et al. (1977), the Yb content of fluorites in biotite granites increases more than 10 times in the latest varieties.

REE-patterns in the different granite groups (Figs. 7 and 8) demonstrate the leading role of crystallization differentiation in their genesis. It is important to point out that LREE are depleted and Yb slightly increased in the slightly albitized and muscovitized biotite granites as compared with the unaltered ones. This fact supports the interpretation that the albite-protolithionite granites may have been generated by metasomatic processes from the other granite types. This is confirmed also by the

marked increase in the Sn, Be, U, and Th content in zones of slight albitization and muscovitization in the biotite and biotite-amphibole granites (Beljaev & Lvov, 1981).

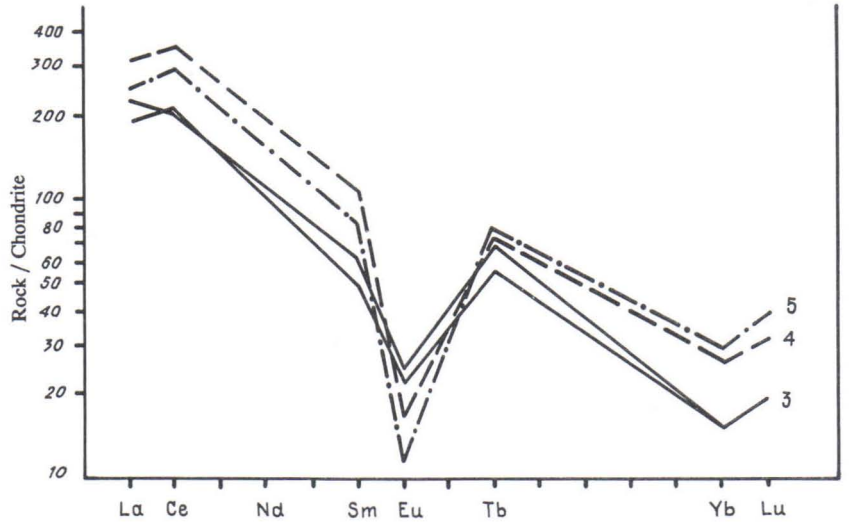


Fig. 7. Chondrite-normalized REE distribution in biotite-amphibole rapakivi granites. Code numbers as in Fig. 5.

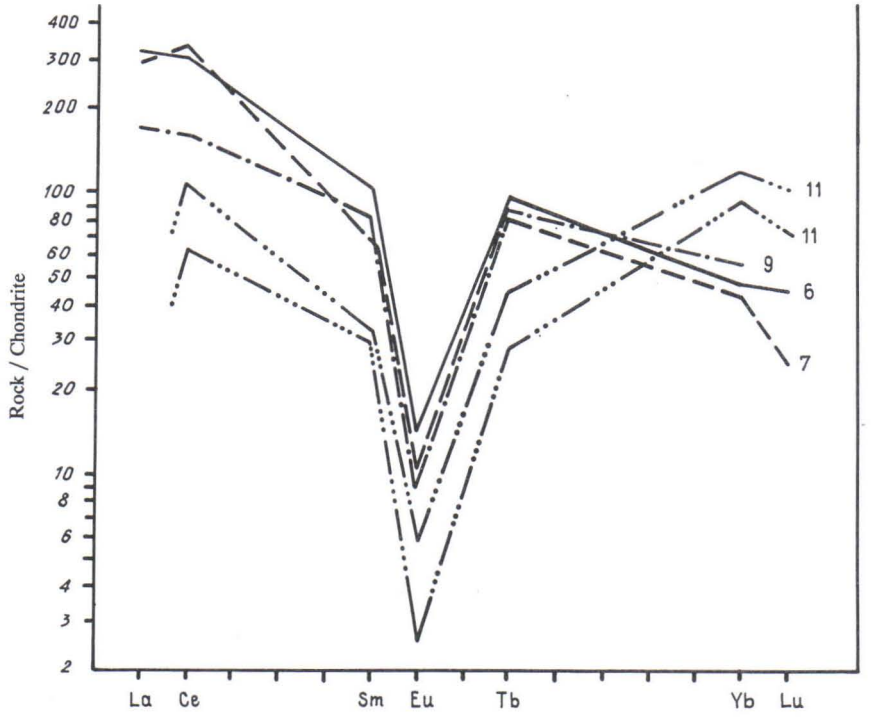


Fig. 8. Chondrite-normalized REE distribution in biotite rapakivi granites. Code numbers as in Fig. 5.

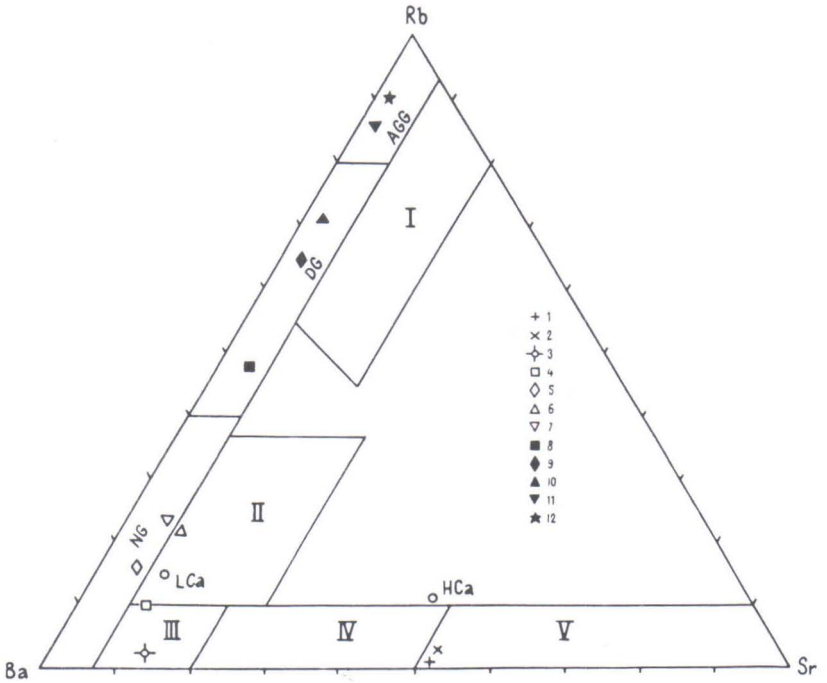


Fig. 9. Composition of the rock types of the granitoids of the Salmi batholith (mean values) in the Ba-Sr-Rb diagram (Kleeman & Twist, 1989). **1**: anorthosite; **2**: monzonite gabbro; **3**: quartz syenite; **4**: wiborgite; **5**: pyterlite; **6**: amphibole-biotite granite aplite; **7**: quartz porphyry dykes; **8**: even-grained biotite granite; **9**: slightly porphyritic biotite granite; **10**: porphyritic biotite granite with fine-grained groundmass; **11**: unequigranular leucocratic dyke granite; **12**: albite-protolithionite granite; I - granites with associated Sn, W, Mo mineralization; AGG - albitized and greisenized granites; DG - differentiated granites; NG - normal granites; II - anomalous granites; III - granodiorites; IV - quartz diorites; V - diorites; LCa - low-calcium granites; HCa - high-calcium granite. Some of the analyses from Shinkarev et al. (1987).

Combined, the rapakivi granites of the Salmi batholith, like those in the other plutons in the East European platform, are characterized by high contents of $SiO_2$, $K_2O$, F, Rb, Y, Nb, Zr, Sn, and REE and low abundances of $Al_2O_3$, CaO, MgO, BaO, and SrO. Elements such as Nb, Sn, Be, U, Th, Y, Rb, Li, and F are strongly enriched in the latest phases. Typically, they also exhibit high Fe/Mg and high K/Na ratio. When compared to the other anorthosite - rapakivi granite complexes of the East European platform the granites of the Salmi batholith are distinguished by their high contents of $SiO_2$, FeO, and $Fe_2O_3$ and low contents of $TiO_2$, $Al_2O_3$, MgO, CaO, and F (Velikoslavinskiy et al., 1978; Vorma, 1976). According to REE data, the main phases of the Salmi batholith are characterized by a higher degree of fractionation than the corresponding granites in the Wiborg batholith (Shinkarev et al., 1987).

The results of a factor analysis of the geochemical data (Fig. 10) show that the evolutionary processes for the granitoids of the Salmi and Wiborg batholits are similar in terms of geochemical features and trends. The rapakivi granites of the Salmi batholith, however, differ from the granites in the Wiborg batholith in their higher contents of $SiO_2$, Na, Nb, and Y (Beljaev, 1985).

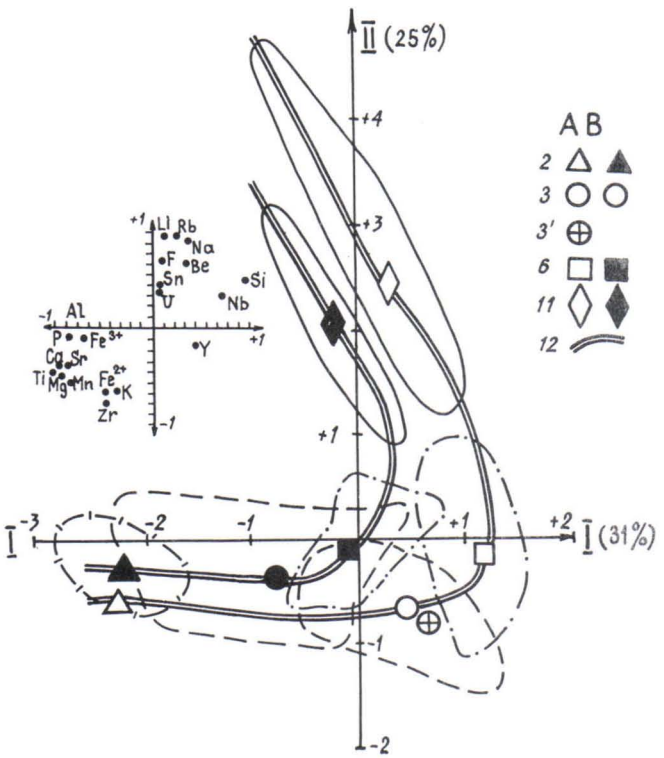


Fig. 10. Results of R mode factor analysis of geochemical data for granitoids of the Salmi (A) and Wiborg (B) plutons. Left: diagram of the factor loadings, level of significance of the factor loadings = 0.21 at the 95 % probability level. Right: diagram of the factor scores (factor weights as %). **2 - 11**: mean compositions of various granitoid types (the same as in Fig. 5); thin solid and dashed lines = boundaries of fields of values for individual samples of corresponding granitoids in A and B. **12**: evolution trend lines for granitoids of the Salmi and Wiborg batholith.

Geochemical studies on contacts of rapakivi granites against the country rocks (Beljaev, 1987) show that both the endocontact and exocontact zones lack significant changes in terms of trace elements distribution, which suggests that the effect of the rapakivi magma on the country rocks was minor at the present level of erosion and that wall-rock contamination of the rapakivi magmas was minor as well.

In the Ab-Or-Qz diagram the mean normative composition of the rapakivi granites of the Salmi batholith falls along the cotectic curve corresponding to $P_{H_2O}$ = 1 kbar (Fig.

11). The compositional points of the biotite granites lie along the curve $P_{H_2O}$ = 1 kbar, while the fine-grained biotite granite dykes plot down to the isobaric minimum $m_1$. These granites obviously crystallized from a residual melt after the biotite granites. The mean normative composition of the albite-protolithionite granites is also near the cotectic curve $P_{H_2O}$ = 1 kbar, close to the minimum point $m_1$. The anchi-eutectic composition of the albite-protolithionite granites might bear witness to their magmatic origin and crystallization from a melt.

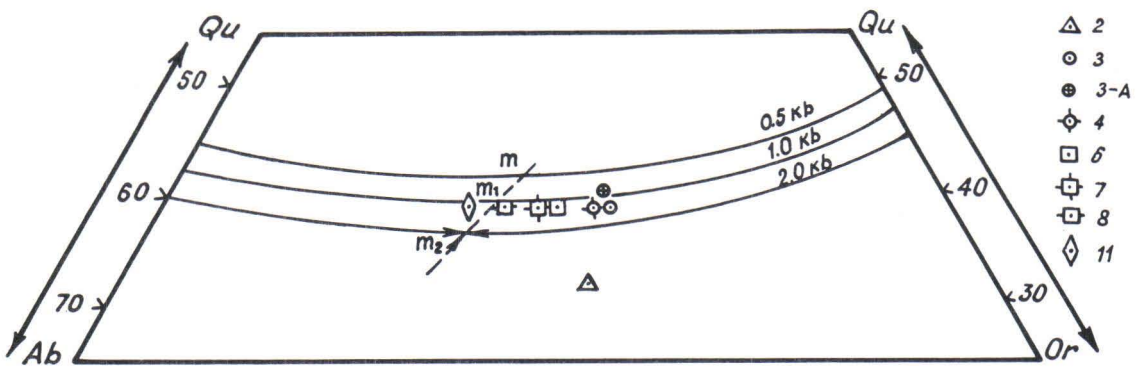


Fig. 11. Normative Ab-Or-Qz diagram of the mean mineral composition of granitoids of the Salmi batholith. Dots correspond to the tripple minima on the cotectic curves at $P_{H_2O}$ = 0.5, 1.0, and 2.0 kbar. Number codes for rock type varieties the same as in Fig. 5. 3-A = normative mode of the granite porphyry from a dyke with xenoliths (see Fig. 31).

The mean normative composition of the quartz syenite lies in the Or field above the cotectic curve of $P_{H_2O}$ = 4 kbar, which may be due to either oversaturation of the quartz syenite melt by the orthoclase component or to their hybridic origin as intermediate rocks between a granite and monzonite.

The tectonic setting of the Salmi batholith, the late lithium-fluorine granites (Sviridenko et al., 1984), the geochemical specialization of the granites high K, Rb, Nb, Y, Zr, REE, F, Sn, Be, and Li and the REE-patterns indicate that the rapakivi granites of the Salmi batholith represent typical subalkaline A-type granites. On the tectonomagmatic diagrams of Pearce et al. (1984) they fall into the field of within-plate granites (Fig. 12), like the granites of the Suomenniemi and Laitila batholits (Haapala & Rämö, 1990).

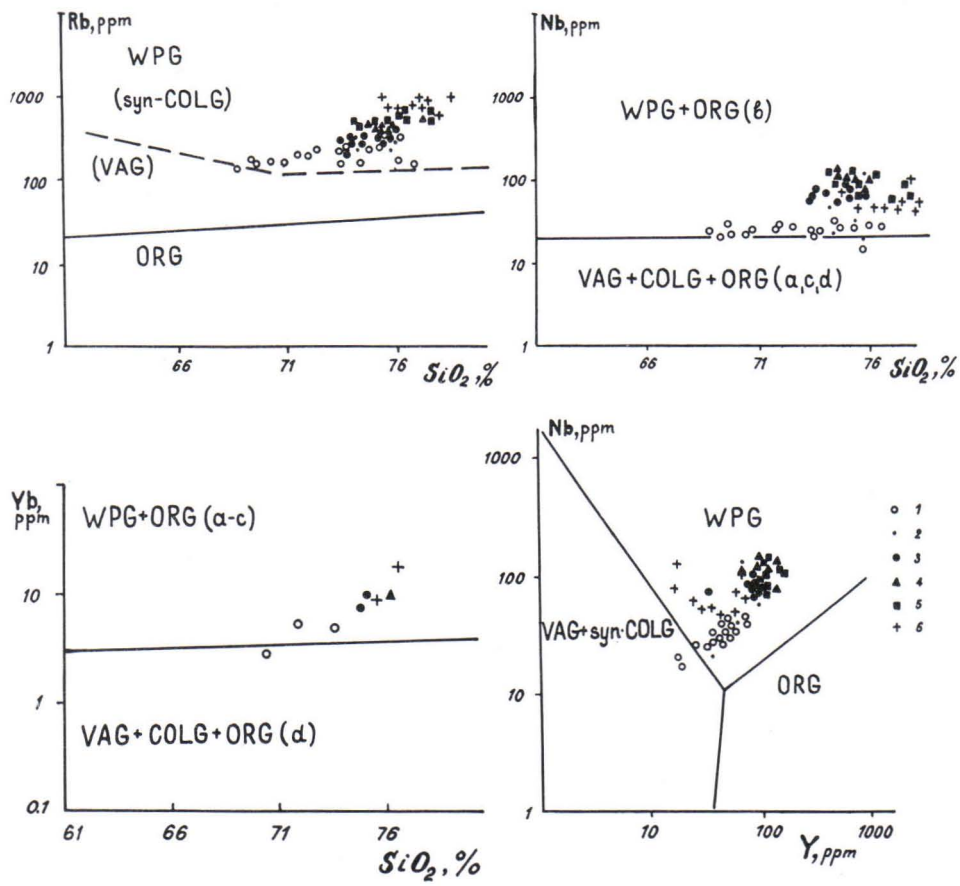


Fig. 12. Analyses of rapakivi granites from the Salmi batholith plotted in the Rb - $SiO_2$, Yb - $SiO_2$, Nb - $SiO_2$, Nb - Y tectonomagmatic discrimination diagrams of Pearce et al. (1984). **1-2**: amphibole-biotite granites: 1 - coarse-grained, 2 - fine-grained vein granites; **3-5**: biotite granites: 3 - even-grained, 4 - porphyritic with fine-grained groundmass, 5 - fine-grained vein granites; **6**: albite-protolithionite granites. ORG - oceanic ridge granites, VAG - volcanic arc granites, WPG - Within-plate granites, COLG - collision granites.

## 4. ORE MINERALIZATION

A number of ore mineralizations of various types are present in the northwestern exocontact of the Salmi batholith, in a locality where the late-stage rapakivi granites are abundant. The mineralizations follow a zone which stretches along the contact of the batholith for about 50 km and has a maximal width of 4 to 5 km. The border of the zone coincides with the line interpreted on the basis of geophysical data to mark a steep flexure in the roof of the rapakivi granites below the country rocks. In the flexure zone the south-western plunge of the roof is changed into a vertical one (Fig. 13). Most of the mineral deposits are concentrated in the central part of the 'zone' in an area where the

roof of the rapakivi complex dips relatively gently below their country rocks. This area in known as the Pitkäranta ore field (Fig. 13).

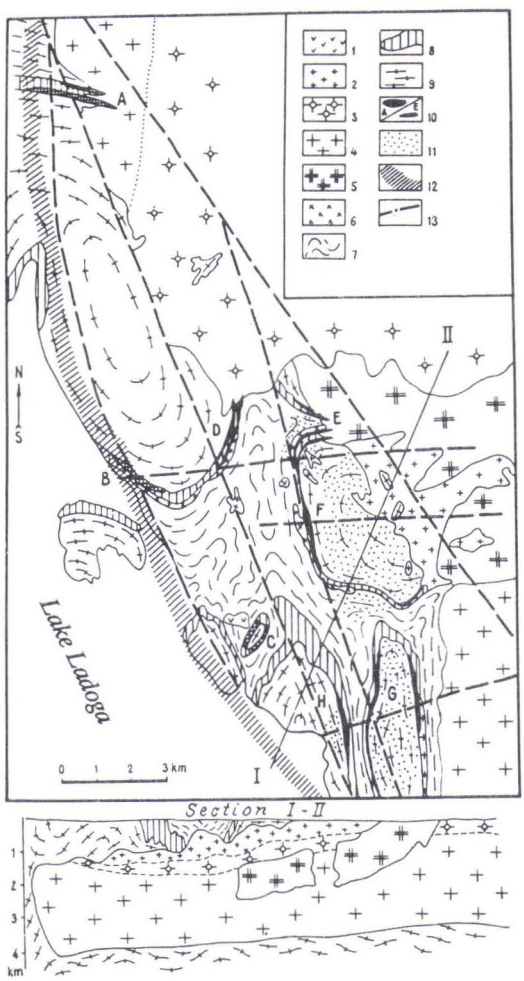


Fig. 13. Geological structure of the Pitkäranta ore district. **1**: Volcanic - sedimentary and intrusive Jotnian rocks; **2-5**: rapakivi granites of the Salmi batholith: 2 - albite-protolithionite granites, 3 - porphyritic biotite granites with fine-grained groundmass, 4 - even-grained biotite granites, 5 - porphyritic biotite-amphibole granites with fine-grained groundmass; **6-9**: Svecokarelian complex: 6 - ceramic pegmatites, 7 - alumina-rich schists of the Ladoga series, 8 - amphibolites and amphibole schists with carbonate horizons (Pitkäranta suite), 9 - granite gneisses of the domes. **10**: deposits: (A-C) tin-polymetallic deposits: A - Kitelä, B - Old Ore Field, C - Heposelkä; (D-H) beryllium-tin-polymetallic deposits: D - New Ore Field, E - Hopunvaara, F - Lupikko, G - Uuksu, H - Ristiniemi; **11**: projection to the recent erosion surface of the dome-like protrusions of the roof of the Salmi batholith consisting of albite-protolithionite granites (depths 70 to 350 m); **12**: projection to the recent erosion surface of the line of a swift flexure in the roof of the Salmi batholith with the plunge changing from gentle to vertical; **13**: disjunctive dislocations.

The main type of ore deposits in the region is represented by skarn deposits with a multi-metal iron, tin, rare metal, polymetal and fluorite mineralization. They are related to the carbonate horizons of the Pitkäranta suite which encloses the gneiss-granite domes. Tantalum mineralization has been encountered in albite-protolithionite granites in the apical parts of the Salmi batholith which are not exposed by erosion and represented. Linear greisen zones carrying Be, Sn, Mo, and Cu mineralization are commonly found within various types of the rapakivi granites and granite gneisses of the domes. Also, placer concentrations of cassiterite were encountered in clastic terrigenous rocks of the Lower Salmi series. Obviously these were originated during erosion of the skarn deposits.

The skarn deposits of the Pitkäranta ore field were first discovered in the beginning of the 19th century. Exploitation in the lodes of the Old Ore Field started in 1814 and continued with some interruptions until 1904. During the 90 year period the mines in the region yielded 100,000 tn Fe; 6,800 tn Cu; 490 tn Sn; and 10.8 tn Ag.

Studies on the deposit started almost immediately after they had been discovered. The first publication is the work by Furman (1812). However, systematical investigations of the deposits of the region were not carried out until the end of the 19th century. The first paper which systematically treated the geology and mineralogy of the Old Ore Field was that by Törnebohm (1891). The next investigation was the fundamental work by Trüstedt (1907), which still remains an outstanding and comprehensive reference for the geology of the deposit. In that work the author gives detailed characteristics of the geological structure of the region, describes the geology and mineralogy of all deposits known at that time, presents views on the genesis and the sequence of the metasomatosis and mineralization, and gives a geological assessment of the region. Eskola (1951) supplemented the work of Trüstedt with his own petrographic and mineralogical studies.

In 1934-1938 the Pitkäranta Corporation company performed revisionary exploration on several deposits in the region. This work resulted in a paper by Palmunen (1939) dealing with assessment of the prospective value of the region.

During 1960-1980 the tin-polymetallic deposit of Kitelä and the beryllium-tin-polymetallic deposit of Uuksu were discovered and explored by the Karelian expedition of the North-western Geological Authority. Prospecting was carried out in all deposits of the region. Important contributions to the exploration and investigation of the deposits of the Pitkäranta ore field were made by Hazov (1967, 1968 etc.).

Among the skarn deposits of the Pitkäranta district two types of deposit groups can be distinguished (Larin, 1980), even though they have gradual transitions: type I beryllium-tin-polymetallic deposits (Uuksu, Lupikko, Hopunvaara, the New Ore Field, Ristiniemi) and type II tin-polymetallic deposits (Kitelä, the Old Ore Field, Heposelkä) (Fig. 13).

The former are situated in the zone above the intrusions of the Salmi batholith with a characteristic rather gentle dip of the roof of the massif. As a rule, they are related to dome-like protrusions of albite-protolithionite granites (Fig. 13), which are found in drill holes at depths between 70 and 350 m. A characteristic feature here is the abundance of fine-grained albite-protolithionite granite dykes and stockscheiders. Type I deposits are characterized by a wide spectrum of the following ore-forming elements: Be, Li, Sn, W, Cu, Zn, Pb, As, Bi, Au, Ag, Cd, In, and Fe. However, only Be, Sn, Cu, Zn, and fluorite are of industrial significance.

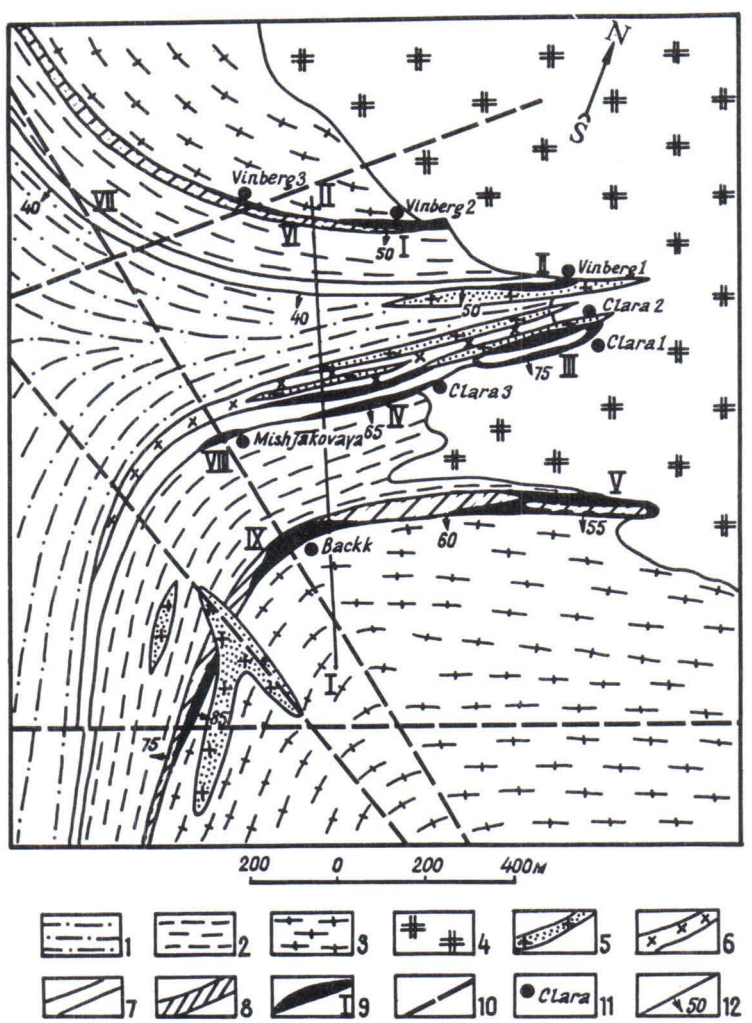


Fig. 14. Geological structure of the Hopunvaara ore deposit. 1: alumina-rich schists of the Ladoga series; 2: amphibolites and amphibole schists of the Pitkäranta suite; 3: granite gneisses of the domes; 4: biotite-amphibole rapakivi granites; 5: albite-protolithionite granites; 6: ceramic pegmatites; 7-8: ore-bearing horizons: 7 - upper, 8 - lower; 9: ore bodies; 10: fractures; 11: mines; 12: dip and strike. I-II - position of the profile.

Type II deposits are usually located near the line marking a sharp flexure of the roof of rapakivi granites with the plunge changing from gentle to vertical. In the area where the roof plunges gently they are located at some distance from the Salmi batholith. The depth of the roof of the rapakivi granites in some deposits is more than 1 km. Dykes of albite-protolithionite granites are either absent or very scarce. A characteristic of deposits of this type is the association of Sn, Cu, Zn, Pb, W, Bi, Ag, Au, Cd, In, and Fe. Only Sn, Cu, and Zn, however, are important on an industrial scale. In terms of size the type II deposits are more significant than the type I deposits.

The ore deposits are predominantly stratiform and concordant with the wall rocks. Only in the zone of the immediate contact with the granites of the Salmi batholith cutting veins, pipes, and irregularly shaped contact bodies are found. As a rule, they have a complex structure due to combination of bodies of ore-bearing metasomatites in various stages of mineralization and facial zonality within "simple" metasomatite bodies.

The following types of ore-bearing metasomatites can be distinguished: magnesian and lime skarns, fluorite-vesuvianite-magnetite metasomatites, aposkarn greisens, propylites and feldspar metasomatites, apodolomite phlogopite-serpentine metasomatites and late carbonate-quartz metasomatites. Outside the contact halo of the Salmi batholith only barren synmetamorphic magnesian skarns are abundant; they differ markedly in composition from the ore-bearing magnesian skarns. The K-Ar age of these rocks is 1950 ± 30 Ma (Shergina et al., 1982).

Magnesian skarns are most wide-spread; they are found predominantly in the upper carbonate horizon and as relicts among lime skarns and later metasomatites (Fig. 15). Sometimes they are found as independent bodies as well. Magnesian skarns host Fe and Zn mineralization, the mineral composition of these rocks is presented in Fig. 16.

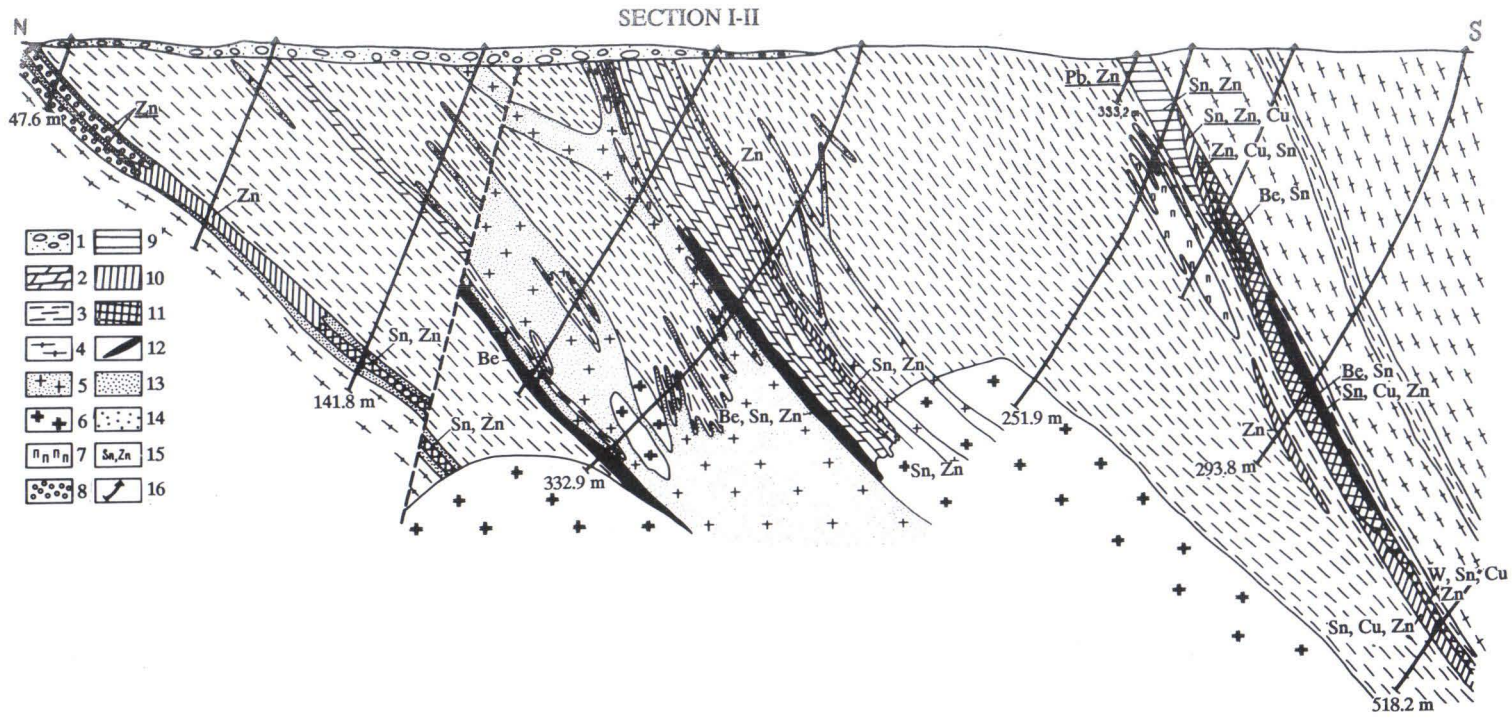


Fig. 15. Geological cross-section along the profile I-II of the Hopunvaara ore deposit. **1**: Quarternary deposits; **2**: marbles and calciphyres; **3**: amphibole schists; **4**: granite gneisses; **5**: albite-protolithionite granites; **6**: biotite-amphibole granites; **7**: ceramic pegmatites; **8**: carbonate-quartz metasomatites; **9-11**: aposkarn propylites: 9 - quartz-chlorite propylites, 10 - epidote propylites, 11 - actinolite propylites; **12**: aposkarn greisens; **13-14**: skarns: 13 - lime skarns, 14 - magnesian skarns; **15**: ore elements (the leading ones underlined); **16**: drill holes.

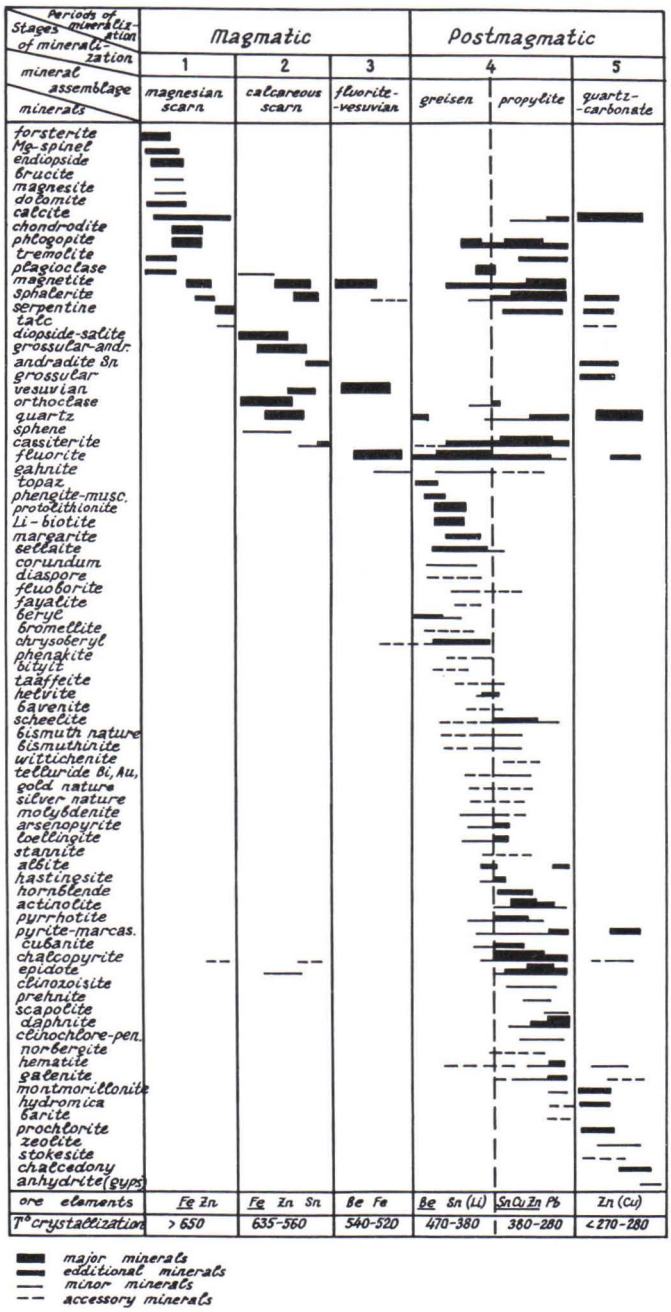


Fig. 16. Paragenesis diagram for the deposits of the Pitkäranta ore district.

Lime skarns (calcareous skarns) are the most widespread metasomatites in the region. They can be divided into exoskarns, generated after primarily carbonatic rocks (magnesian skarns and calciphyres), and endoskarns as well as rocks adjacent to skarns (rocks containing feldspars), generated by replacement of aluminium silicate rocks (mainly amphibole rocks interlayering with marbles in the carbonate horizons of the Pitkäranta suite). The mineral composition of the rocks is illustrated in Fig. 16. Related to lime skarns there occurs syngenetic Fe-Zn and Sn mineralization. Most part of the Sn is dispersed diadochically in garnets (Fig. 17) but cassiterite is present as well. The Sn

content in garnet I ($Andr_{30-82}Gross_{18-70}$) varies between <0.05 and 0.87 % (Figs. 17 and 18). The later garnet II of andradite composition constitutes monomineral lenses, interlayers and drusy nests in the skarn. It is fairly enriched in Sn (0.51-2.20 %) (Fig. 17 and 18). The latest garnet III is developed in the post-skarn stage and is related to the formation of the late carbonate-quartz metasomatites. It is characterized by a very strong compositional zoning and extremely low Sn contents (<0.05 %) (Figs. 17 and 18). The lime skarns are characterized by district metasomatic zonality as illustrated in Table 1.

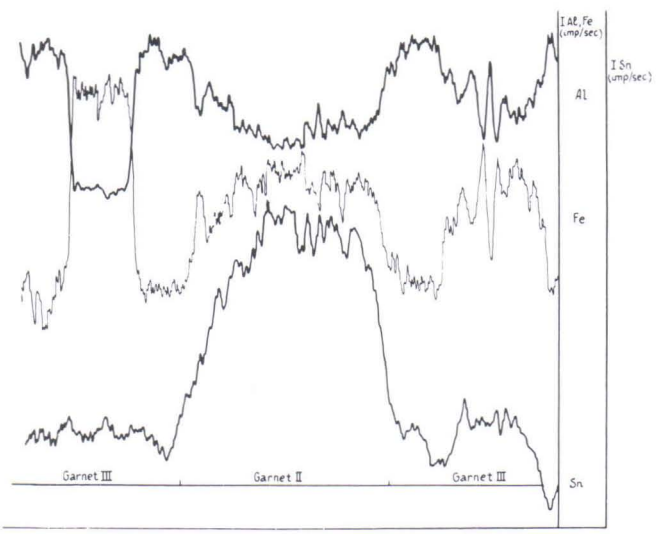


Fig. 17. Concentrations of Fe, Al, and Sn in a profile across a zoned garnet crystal from the Kitelä deposit. Linear scale: 1 cm = 100 $\mu$m.
max Fe = 17.9 %, max Al = 4.6 %, max Sn = 1.05 %,
min Fe = 12.1 %, min Al = 0.54 %, min Sn = 0.05 %.

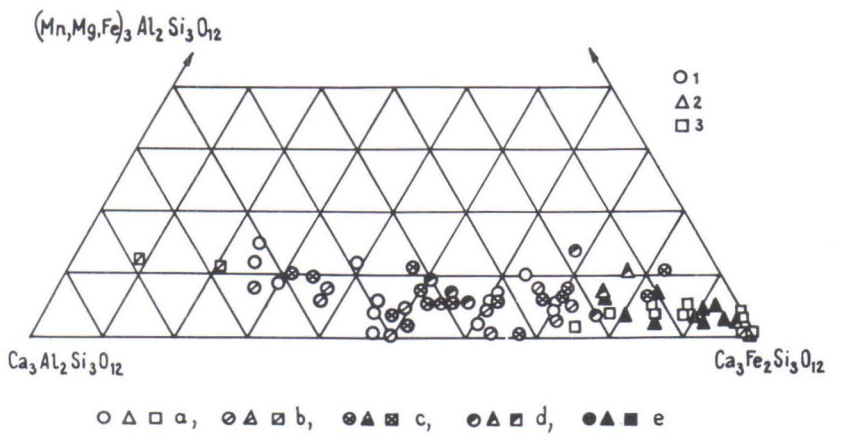


Fig. 18. Chemical composition of garnets from lime skarns and aposkarn metasomatites from the Kitelä deposit. 1-3: generations of the garnets; a-e: tin contents in garnets (in wt-%): a - <0.05, b - 0.05-0.2, c - 0.2-0.6, d - 0.6-1.0, e - >1.0.

Table 1. Metasomatic column for the bi-metasomatic skarns in the Kitelä deposit.

| Zones | | Endoskarns and skarn-neighboring rocks | | | | | Exoskarns and calcifyres | | | |
|---|---|---|---|---|---|---|---|---|---|---|
| | | Feldspa-thized schists | Quartz-feldspar | Pyroxene-garnet-feldspar | Feldspar-pyroxene-garnet | Garnet | Pyroxene-magnetite | Pyroxene-garnet | Pyroxene | Calcifyres |
| Rock-forming minerals | Main | Amphibole biotite, quartz, orthoclase, plagioclase | Quartz, orthoclase, plagioclase | Orthoclase, pyroxene, garnet | Pyroxene, garnet | Garnet | Pyroxene | Pyroxene, garnet | Pyroxene | Dolomite, calcite |
| | Accessory | Chlorite, pyroxene, sphene | Pyroxene, garnet, sphene | Quartz, plagioclase, sphene | Orthoclase, sphene | Pyroxene, calcite, sphene | Garnet | | Garnet, calcite | Pyroxene, garnet, phlogopite, serpentine |
| Ore minerals | Main | | | | | | Magnetite, marmatite | | | |
| | Accessory | | | Cassiterite | Cassiterite | Cassiterite | Cassiterite | Magnetite, cassiterite, marmatite | Magnetite | |
| Ore elements | Main | | | | Sn | Sn | Fe, Zn, Sn | Sn | | |
| | Accessory | | | Sn | | | | Fe, Sn | Fe, Sn | |

Fluorite-vesuvianite-magnetite metasomatites are distributed exclusively within the type I deposits. They form both concordant stratiform bodies and vein-like or pipe-like bodies that sometimes branch in a complicated way. Characteristic features are rhythmically banded, frilly, and concentric textures. Related to these rocks is Be mineralization; almost all Be occurs diadochically in vesuvianite. Unlike the vesuvianite in the skarns, the one in these metasomatites is strongly enriched in Be (up to 0.85 %) and F (0.77-1.23 %).

The aposkarn greisens (Fig. 16) are found exclusively within the type I deposits. As far as the time of their formation is concerned, they are separated from the previously described ore-bearing metasomatites by the intrusion of rapakivi granite dykes. Haloes of greisenization in skarns are frequently seen around dykes of albite-protolithionite granites. Related to greisens is tin, beryllium, lithium, and fluorite mineralization. The aposkarn greisens have a zonal texture and commonly constitute united zoned bodies with aposkarn propylites (Table 2). In the Uuksu deposit, where the apical protrusions of albite-protolithionite granites are at the smallest depths (ca. 100 m), greisenization is most intense. Dominating here are greisen bodies made up of metasomatites of the inner part of the metasomatic column (Table 2). Usually, the propylitic zones are reduced to a minimum. Again in deposits with deeper location of the domes of these granites (Lupikko, Hopunvaara) the rear parts of the metasomatic column are reduced. Here the aposkarn greisens are predominantly of fluorite-mica composition and are surrounded by a wide halo of aposkarn propylites.

Aposkarn propylites (Fig. 16) occur in all deposits in the region. Related to them is the main part of the tin-polymetallic mineralization. In the type II deposits they form slightly zoned bodies of considerable extent, with predominant amphibole propylites.

Phlogopite-serpentine aposkarn metasomatites occur almost exclusively in the upper carbonate horizon. They are closely associated with the aposkarn propylites and are practically identical with them in terms of mineralization, ore minerals, and their typomorphical characteristics.

The late carbonate-quartz metasomatites are present in all deposits in the region, but are volumetrically minor. The copper-zinc and, less commonly, tin mineralizations in these rocks have been recrystallized.

Table 2. Combined metasomatosis column for aposkarn, greisen, greisen-propylite and propylite bodies.

| Zones | | Topaz-quartz | Fluorite-topaz-mica | Fluorite-mica | Fluorite-feldspar | Amphibole | Phlogopite-epidote | Quartz-chlorite |
|---|---|---|---|---|---|---|---|---|
| Rock-forming minerals | Main | Topaz, quartz | Fluorite, topaz, Li-biotite, protolithionite | Phlogopite, fluorite, sellaite, gahnite, corundum | Plagioclase ($An_{21-50}$), albite, orthoclase, fluorite | Actinolite, hornblende | Epidote, phlogopite, actinolite, tremolite, quartz, calcite, clinozoisite | Daphnite, quartz, calcite, phlogopite, epidote |
| | Accessory | Muscovite, protolithionite fluorite | Margarite, gahnite | Diaspore, fluorite, fayalite, Li-biotite, margarite, hastingsite | Hornblende, hastingsite, phlogopite, gahnite, quartz, fluoborite, corundum | Phlogopite, epidote, hastingsite, quartz, fluorite, calcite, gahnite | Fluorite, prehnite, daphnite | Scapolite, albite, tremolite, actinolite, prehnite |
| Ore minerals | Main | Beryl | Chrysoberyl | Chrysoberyl | Cassiterite, helvite group, phenakite, arsenopyrite, löllingite | Cassiterite, chalcopyrite, sphalerite, pyrrhotite, magnetite | Cassiterite, sphalerite, chalcopyrite, pyrrhotite, pyrite, magnetite | Galena, sphalerite, cassiterite, hematite, mushketovite, magnetite, pyrite |
| | Accessory | Chrysoberyl, cassiterite | Beryl, cassiterite | Helvite group, brommelite, bitheite, taaffeite, cassiterite, scheelite, löllingite, arsenopyrite | Chalcopyrite, cubanite, sphalerite, pyrrhotite, scheelite, bismuthite, tellurides, Au, Ag, Bi | Pyrite, cubanite, galena, bismuthite, molybdenite, tellurides, stannite, scheelite, Au, Ag, Bi | Galena, scheelite | Chalcopyrite |
| Ore elements | Main | Be | Be | Be | Sn, Be | Sn, Cu | Sn, Zn, Cu | Pb, Zn, Sn |
| | Accessory | Sn, Li | Sn, Li | Sn, W | Zn, Cu, W, As | Zn, W, As | W, Pb | Cu |

The spatial-temporal interrelations between mineral parageneses in the ore-bearing metasomatic and magmatic rocks, as well as the physico-chemical conditions of mineralization were subjected to study to assess the sequence of stages and steps in the mineral deposition. Two stages of mineralization were distinguished, synmagmatic and postmagmatic. In both stages several (interchanging) mineralization events occur (Fig. 16). The metasomatites of the first stage were generated at a time when the rapakivi magma was not yet crystallized. This is verified by intersection of the skarns by the rapakivi granites, by the existence of xenoliths of tin-bearing lime skarns in an apophysis of the rapakivi granite, and by practically a total lack of endoskarns after rapakivi granites. Generation of ore-bearing metasomatites of the second stage took place after the crystallization of the rapakivi granites and it is closely related to the post-magmatic alteration in rapakivi granites, most intensively manifested in the apical parts which consist of albite-protolithionite granites. This is demonstrated by the Be, Sn, Cu, and Zn mineralization around granite dykes intersecting the skarns. Moreover, zonality in these "dyke-neighboring" metasomatites is identical to the zonality in the aposkarn greisen - propylite bodies discussed above.

The ore deposits show low-contrast zoning along the ore-controlling NW-SE and E-W-trending faults and, in contact-neighboring ore bodies, parallel to the contacts. Lateral zonality across the deposits is practically always of a high-contrast asymmetrical monodirectional character. In the lower carbonate horizon, where most of the ore deposits are located, zonality appears in respect to the contact of this horizon against the granite gneisses of the domes (Fig. 19). In the contact zone of the batholith zonality always appears along rapakivi granite contacts.

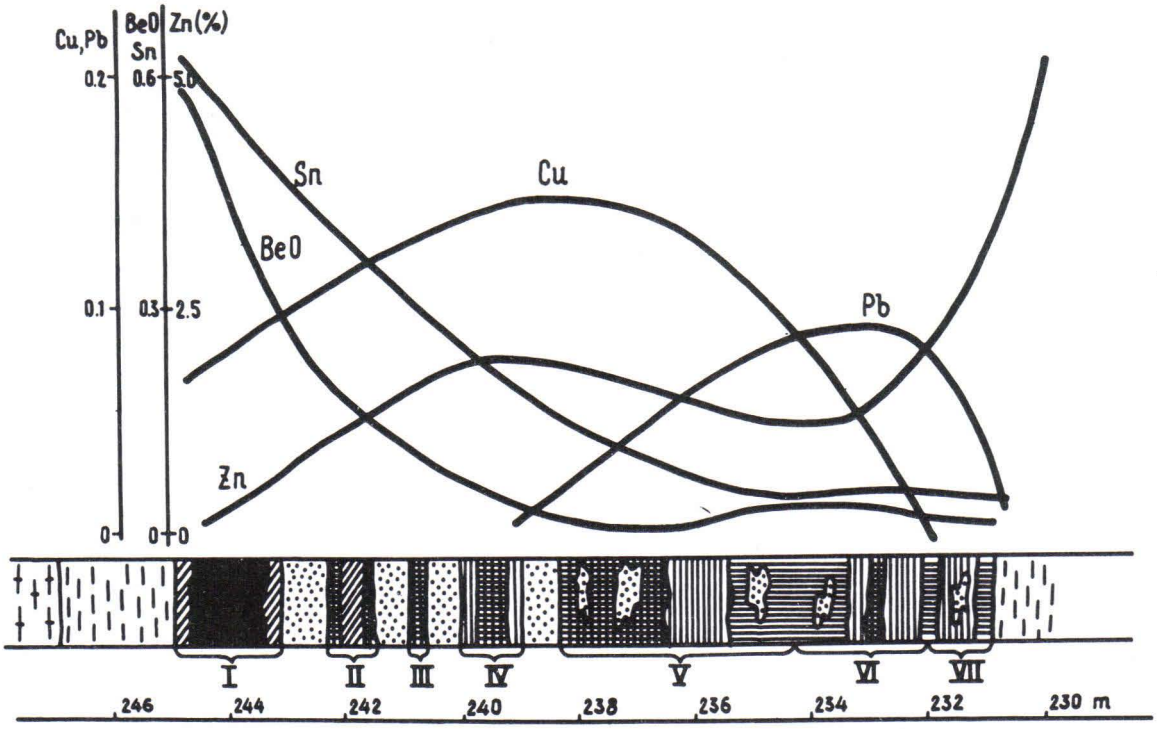


Fig. 19. Variation trends in the mineralization in a cross-section of the Lupikko ore deposit (lower carbonate horizon), illustrating an one-way mineralization and metasomatic zonality. Legend is the same as in Fig. 15.

The vertical zonality is generally symmetricant divergent. In some cases both normal and inverse zonality can be seen (Fig. 15, 20). In type I deposits it appears to be of higher contrast than in type II deposits. The general sequence of zonality for the former is: **Be**, Li, Sn - (Be), Sn, W, (As), Cu, Zn - Sn, Cu, Zn, (Pb), - (Cu, Zn), Pb, and for the latter: **Sn - Sn, Cu**, (Zn) - Cu, Zn - Zn. The ore zonality is related to the zonality of metasomatic rocks, especially in the second-stage metasomatites (Figs. 19, 21, 22).

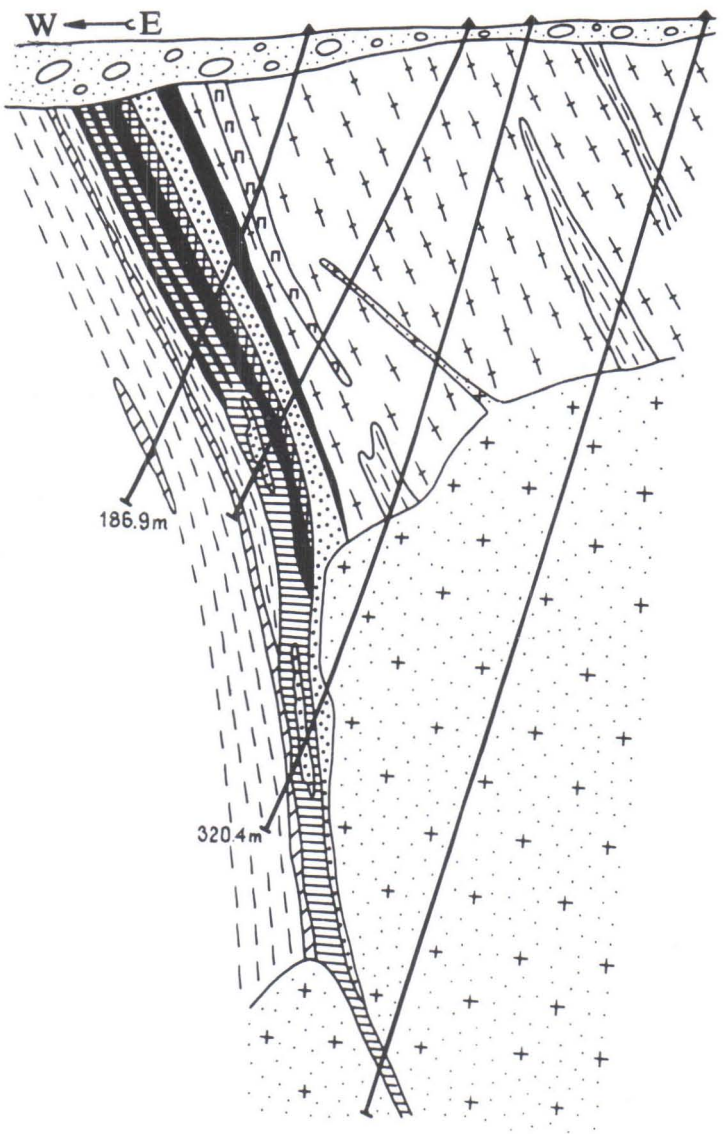


Fig. 20. Cross-section over the ore body of the Uuksu deposit, illustrating a reverse vertical metasomatic zonality. Legend is the same as in Fig. 15.

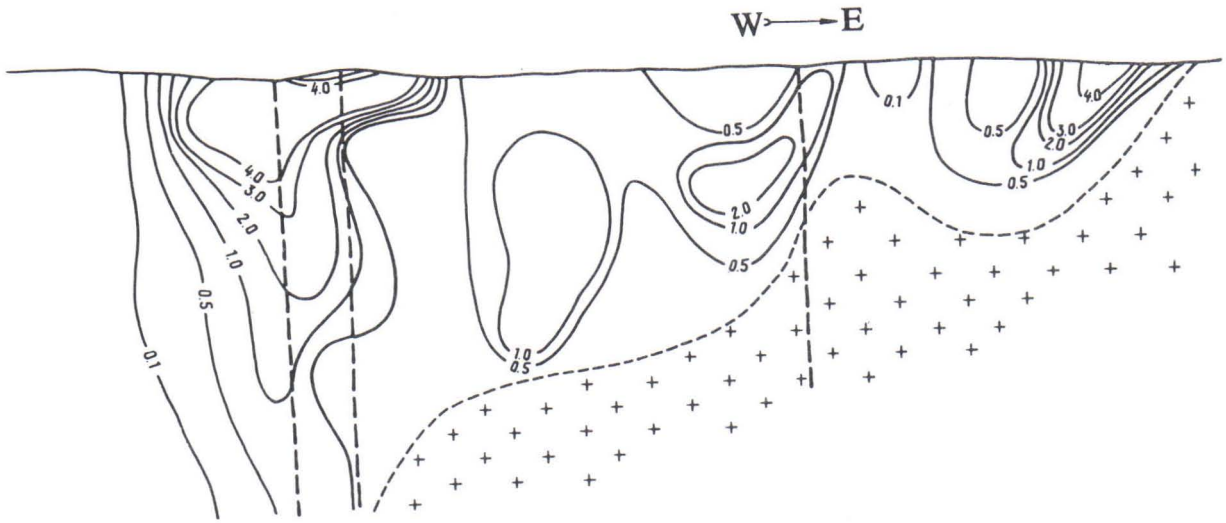


Fig. 21. Distribution of tin (in m-%) in the plane of the vertical projection of the lower carbonate horizon in the Kitelä deposit.

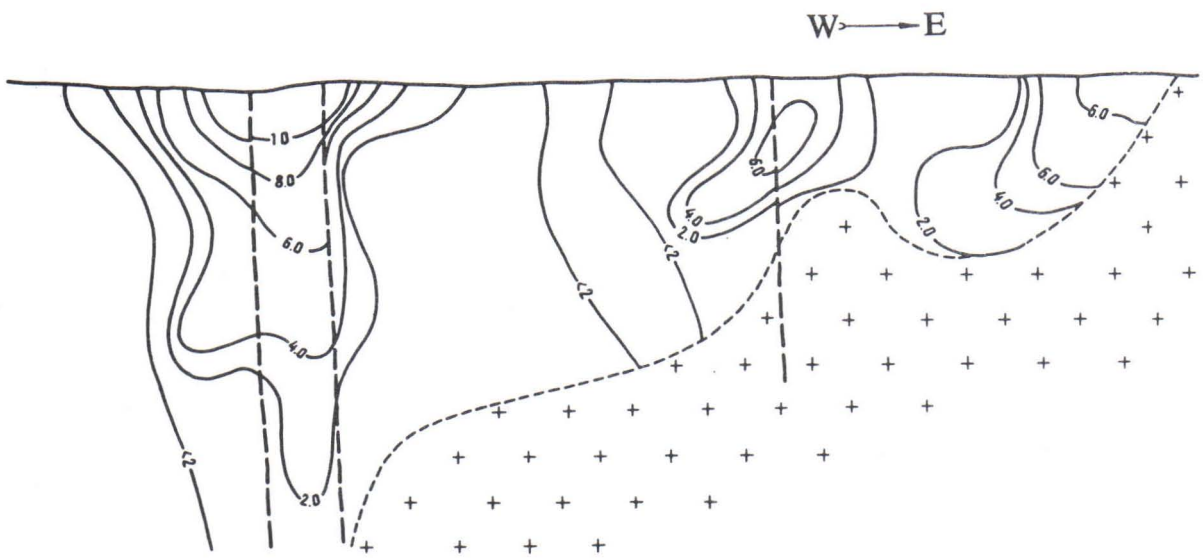


Fig. 22. Distribution of aposkarn prophylites is given in the plane of the lower carbonate horizon in the Kitelä deposit (total thickness in the sections).

It is worth mentioning that the centres of the ore deposits, marked by a symmetrical vertical zonality, lie practically at the same hypsometric level in most deposits of the region. This level controls the richest ore mineralization in all types of deposits. This is

also where the Sn and Be-Sn ore pipes are located; they have a tendency to lie subhorizontally in the plane of the carbonate horizons. Spreading of the mineralization is seen extending from the steeply dipping ore-bringing channels along dislocations within the carbonate horizons (Figs. 21 and 22). Going towards the Salmi batholith, the orientation of the ore pipes gradually turns into one which is subparallel to the roof of the batholith.

Regarding the Pitkäranta ore field as a whole, zonality is manifested as follows: going from southeast to northwest, as the depth of the apical protrusions of albite-protolithionite granites is increased, the beryllium-tin-polymetallic deposits gradually change to tin-polymetallic ones. In this context the role of the first elements (Li, Be) and the last ones (Pb) in the ore metal sequence is diminished and the role of the intermediate ones (Sn, Cu) increased in the deposits of the first type. The set of the metasomatites is changed as well as is their ore content. The role of the aposkarn greisens and fluorite-vesuvianite-magnetite metasomatites is gradually reduced, and the role and the ore potential of the propylites (especially the amphibole ones) is strengthened, as is the ore potential of the lime skarns. The high-contrast encountered between the zonality of the ores and metasomatic rocks is reduced, and the depth of mineralization is increased down to 700 m.

## 5. GEOCHRONOLOGY OF THE ROCKS OF THE SALMI BATHOLITH

Geochronological investigations on the granites of the Salmi batholith were carried out by Shergina et al. (1982), using the Pb-Pb on zircon, K-Ar on amphibole and mica, and Rb-Sr on whole rock. Based on these investigations it was concluded that all rapakivi granite phases were synchronous within an age bracket of 1550 ± 30 (1$\sigma$) Ma. New data on the geochronology of the Salmi batholith, acquired at the Institute of Precambrian Geology and Geochronology, are presented in Table 3; they include U-Pb zircon determinations and Sm-Nd and Rb-Sr mineral datings both from the granites and from the basic rocks. Ages were calculated using the ISOPLOT program (Ludwig, 1988); errors are given at the 95 % confidence level.

Table 3. Isotopic ages of rocks from the Salmi batholith and the Pitkäranta ore district.

| Rocks (ores) type | Dating method | Age (Ma) | ± 2σ (Ma) |
|---|---|---|---|
| Anorthosite | U-Pb / apatite | 1566 | 4 |
| | Sm-Nd / rock forming minerals and whole rock | 1552 | 69 |
| I phase rapakivi granite | U-Pb / zircon | 1543 | 8 |
| | Sm-Nd / amphibole, apatite, bastnaesite and whole rock | 1560 | 45 |
| | Rb-Sr / rock forming minerals and rocks | 1455 | 17 |
| III phase rapakivi granite | U-Pb / zircon | 1517 | 47 |
| Lime skarn | Sm-Nd / rock forming minerals | 1546 | 20 |
| Aposkarn greisen | Sm-Nd / rock forming minerals | 1491 | 42 |

Zircons from the phase I rapakivi granites (pyterlites, Fig. 23) are characterized by slightly discordant U/Pb relations and they define a discordia with an upper intersection of 1543 ± 8 Ma. Zircons from the phase III granites (fine-grained porphyritic biotite granites) are more discordant and give an upper intercept age of 1517 ± 47 Ma (Fig. 23). The Sm-Nd whole rock and high-REE minerals (amphibole, apatite, bastnaesite) isochron from three samples of phase I pyterlites corresponds to an age of 1560 ± 45 Ma, with an initial $\varepsilon_{Nd}$ value of -6.9.

The Rb-Sr whole rock data formerly obtained for various granite phases (Shergina et al., 1982) do not form a single isochron and the apparent Rb-Sr ages for the later phases are lower than the Pb-Pb and K-Ar ages, which is interpreted being due to prolonged postmagmatic processes (Shergina et al., 1982). A similar case has been observed in the Nordingrå rapakivi batholith (Welin & Lundqvist, 1984) and in postorogenic Svecokarelian granitoids in Finland (Welin et al., 1983). The age of the postmagmatic processes in the Salmi batholith is estimated by the authors to be 1455 ± 17 Ma based on a Rb-Sr mineral isochron from a phase I pyterlite sample.

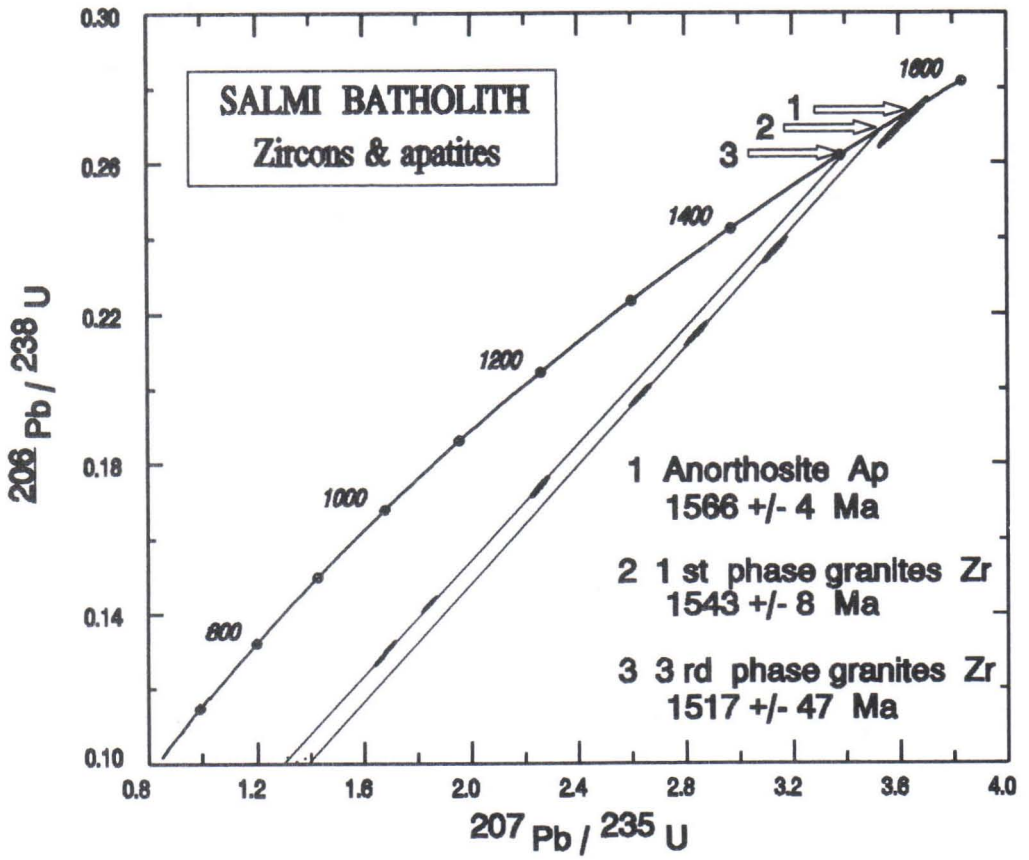


Fig. 23. U-Pb concordia plot for apatites from anorthosites and zircons from rapakivi granites (first and third phases) of the Salmi batholith.

Apatites separated from two anorthosites have an almost concordant U-Pb age of 1566 ± 4 Ma, while the internal Sm-Nd isochron corresponds to an age of 1552 ± 69 Ma, and an initial $\varepsilon_{Nd}$ value of -6.8.

The above data are indicative of a time gap of at least 10 Ma between the crystallization of the anorthosites and the phase I rapakivi granites. Such a time gap is comparable to the duration of emplacement of the Wiborg batholith as determined by U-Pb on zircons (Vaasjoki et al., 1991). The time gap between the crystallization of the main intrusive phases in the Salmi batholith and the completing of postmagmatic processes or the cooling of the massif accompanied by closing of the Rb-Sr isotope systems in minerals is about 100 Ma.

## 6. GEOCHRONOLOGY OF THE ORES IN THE PITKÄRANTA ORE DISTRICT

Various stages of mineralization in the Pitkäranta district have been dated by the Sm-Nd method (Amelin et al., 1990). An isochron of a lime skarn (two generations of garnet, clinoenstatite, diopside, and the whole rock) corresponds to an age of 1546 ± 20 Ma, with an initial $\varepsilon_{Nd}$ value of -10.6 (Fig. 24). An isochron from an aposkarn greisen (fluorite, topaz, oligoclase, muscovite, protolithionite, and whole rock) corresponds to an age of 1491 ± 42 Ma, and initial $\varepsilon_{Nd}$ value of -7.4 (Fig. 25).

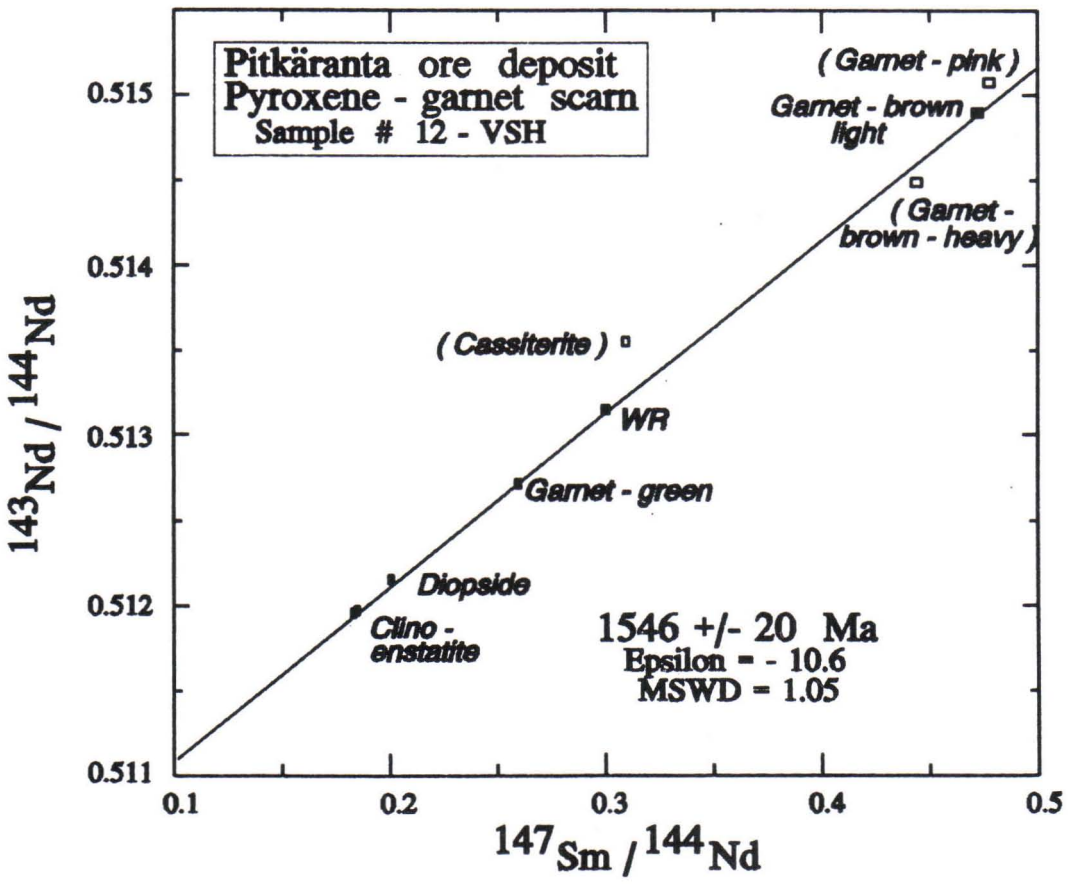


Fig. 24. Sm-Nd isochron plot for a lime skarn from the Pitkäranta ore district. Minerals listed in parentheses not included in the isochron calculation.

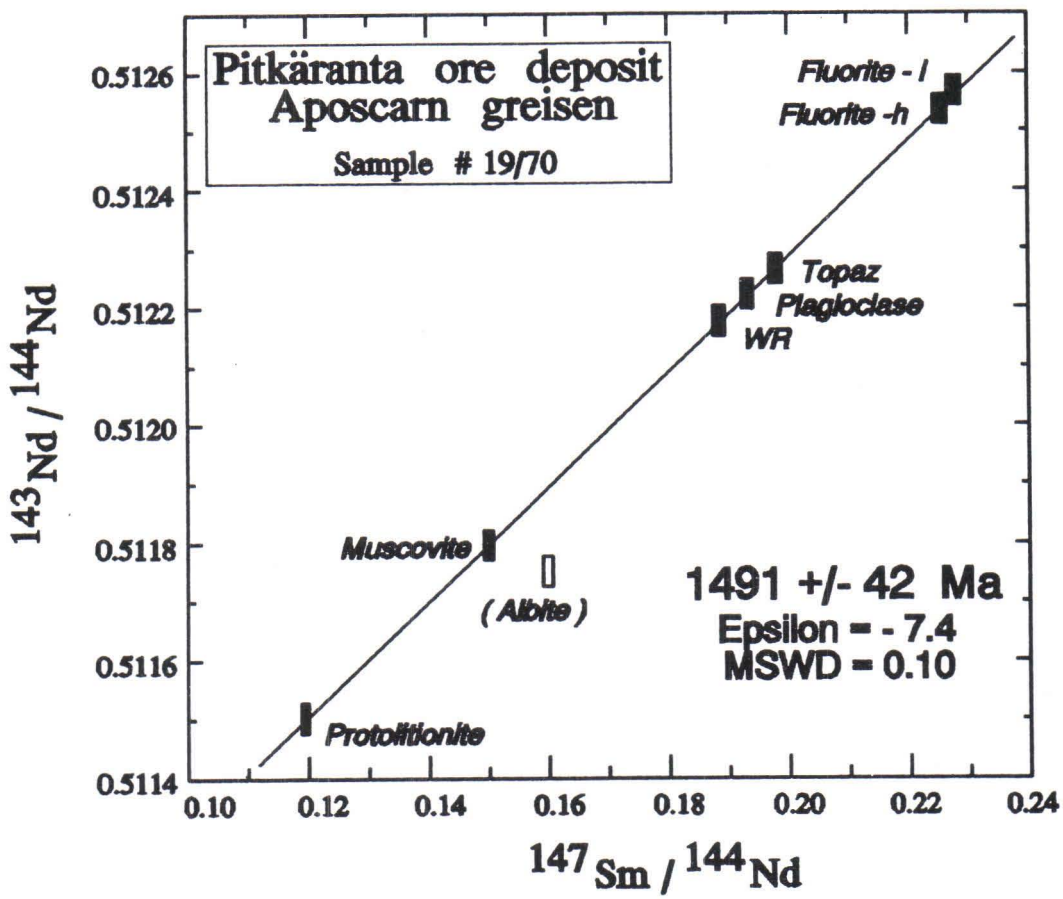


Fig. 25. Sm-Nd isochron plot for an aposkarn greisen from the Pitkäranta ore district. Albite point is not included in the isochron calculation.

The age data of the skarn coincide with the age of the phase I rapakivi granites, while the $\varepsilon_{Nd}(T)$ value is essentially different from the $\varepsilon_{Nd}(T)$ of the rocks of the Salmi batholith being intermediate between the latter and the $\varepsilon_{Nd}(1550\ Ma)$ value -12.9 of the granite gneiss in the country rock. These data support the assumption that the ore-forming process of the first stage has been related to the emplacement of the main phases of the Salmi batholith and included material from the country rocks in the process.

The age and $\varepsilon_{Nd}$ value of the aposkarn greisen imply that the metasomatites of the second stage are separated in time from the crystallization of the main intrusive phases of the Salmi batholith, but that their material may have been derived from the batholith during postmagmatic processes.

## 7. ISOTOPE GEOCHEMISTRY

Lead isotopic compositions of feldspars from the Salmi batholith and from galenas from the ore deposits in the Pitkäranta ore district (Larin et al., 1990) are presented in Fig. 26. The feldspars were treated by acid leaching in order to remove the phases containing uranium and radiogenic lead. The points for galenas and feldspars form a single compact cluster with the model parameters (Stacey & Kramers, 1975) as follows: low values of $\mu_2$ = 8.6 to 9.2 and high of $\kappa_2$ = 4.1 to 4.5 as well as old model ages of 1.8 to 2.0 Ga. These data are indicating of a lower crustal source for the lead in the whole rocks and ores.

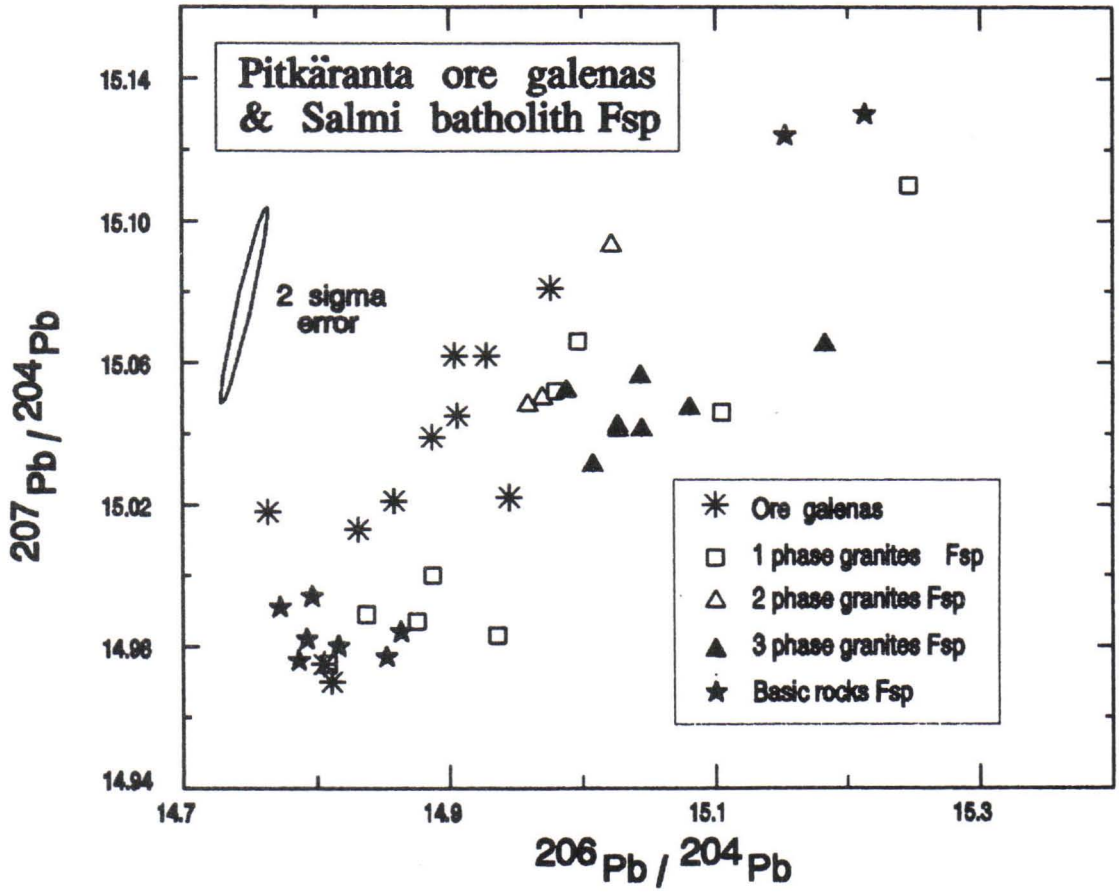


Fig. 26. Lead isotope composition of ore galenas from the Pitkäranta ore district and of feldspars (orthoclase and oligoclase) from the rapakivi granites, monzonites, anorthosites, and gabbronorites the Salmi batholith. Feldspars were leached with $HNO_3$ in order to remove the phases containing U and radiogenic Pb.

The neodymium $T_{DM}$ model ages for the basic and acidic rocks lie in the interval of 2730-2850 Ma, when calculated using a two-stage model (Liew & Hoffman, 1988) with

the assumption that the ratio $^{147}Sm/^{144}Nd$ in the protolith of the Salmi batholith was equal to the model value for the entire Archean continental crust, 0.1285 (Taylor & McLennan, 1985). The Rb/Sr ratio in the protolith, as calculated from the mean $T^{Nd}_{DM}$ = 2790 Ma and $I_{Sr}$(1550 Ma) = 0.7052-0.7057, is 0.086 ± 0.005, which is slightly lower than the model Rb/Sr ratio of the entire Archean continental crust (0.130) but higher than the model Rb/Sr ratio of the lower crust (0.023) (Taylor & McLennan, 1985).

The Nd, Sr, and Pb isotopic data point to a Late Archean crustal protolith both for the granites and for the basic rocks of the Salmi batholith, and suggest a genetic relation between the granites and the ores. The $\varepsilon_{Nd}$(T) values for the Salmi batholith (-6.5 to -7.8) lie between the $\varepsilon_{Nd}$(1550 Ma) values for the rocks hosting the Salmi batholith (-4.8 for the Early Proterozoic schist of the Ladoga series and -12.9 for the granite gneiss from the Kokkaselkä dome). However, the lower values of $I_{Sr}$(1550 Ma) in the rocks of the Salmi batholith as compared with $I_{Sr}$(1550 Ma) in the host rocks (0.7088 for granite gneiss and 0.7274 for schist) are in contradiction with the assumption that the material of the Salmi batholith was derived by mixing of Archean and Proterozoic upper crustal rocks. These obtained isotopic characteristics do not contradict the model of mixing of material from the Archean lower crust and from the depleted mantle, assuming that the proportion of the crustal component is not less than 50 % (Neymark et al., in prep).

## 8. GENESIS OF THE PARENT MAGMA OF THE SALMI BATHOLITH

The problem of the genesis of the anorthosite - rapakivi granite assemblage is complicated and it has not been adequately resolved up to the present time. One of the key questions is the relation of the gabbro-anorthosite complexes and the rapakivi granite batholiths. At present, three main hypotheses on the problem exist:

1. Gabbro-anorthosites and rapakivi granites are genetically unrelated and have distinct sources (Sudovikov, 1967; Sviridenko, 1968; Vorma, 1976).
2. Gabbro-anorthosites and the rapakivi granites are cogenetic but not comagmatic. This is a hypothesis supported by most petrologists studying these rocks (Barker et al., 1975; Emslie, 1985; Fountain, 1981; Anderson, 1983; Nurmi & Haapala, 1986; Haapala & Rämö, 1990).
3. Gabbro-anorthosites and rapakivi granites are comagmatic and have a single source. This model is presented in the papers by Velikoslavinskiy et al. (1978), Shinkarev and Ivannikov (1983), Sharkov (1974), Bogatikov et al., (1985), Birks and Koshik (1984), Higgins and Doig (1981). Differences in the opinions of these authors are related to

assumptions on the composition of the initial magma, the mechanism of its generation, and the character of its subsequent evolution.

The geochronological and isotope geochemical data on the Salmi batholith show that the gabbro-anorthosites and rapakivi granites are practically coeval and have identical initial Nd, Pb, and Sr isotope composition. This does not contradict with the assumption of a single source for these rocks and could prove their comagmatic character. The minor but yet significant difference in the age of the anorthosites and the rapakivi granites of the main intrusive phase (ca. 20 Ma.), as well as the possibly still younger age of the latest rapakivi granites, are most probably caused by the long duration of the evolution of the magmatic system that generated the Salmi batholith.

Another important problem regarding this rock assemblage is the question about the source of the material. As mentioned above, most of authors tend to accept a lower crust at source for the rapakivi granites and a mantle source for the basic rocks. Barker et al. (1975) suggested a model which implies that a convecting alkali olivine basalt magma produces the gabbro-anorthosite complex. Interaction of this magma with the lower crust formed a secondary magma of quartz syenite composition that produced the mangerite-syenite complexes. Interaction of this secondary melt with the material of the middle crust originated a new, more sialic magma from which the potassium-rich biotite and biotite-amphibole granites (rapakivi granites) crystallized. Bridgwater and Windley (1973) explain the generation of the anorthosite - rapakivi granite assemblage in a slightly different way. According to their model the gabbro-anorthosites are produced from mantle-derived basaltic magma and the rapakivi granites from a magma generated by the influence of a mantle diapir on the material of the lower crust. Some authors (Velikoslavinskiy et al., 1978; Higgins & Doig, 1981) suggest the upper mantle to be the source for all rocks in the assemblage. Further, there are conceptions that the primary magma was generated as a result of mixing of a mantle-derived basaltic magma and a secondary anatectic magma originated by partial melting of a lower-crust material (Kranck, 1969; Shinkarev & Ivannikov, 1983; Sharkov et al., 1983, etc.). Fairly exotic conceptions on the genesis of the rapakivi are presented by Levkovskiy (1975). According to this author, rapakivi granites are products of postmagmatic metasomatic replacement of basic intrusions.

The data on the Nd, Sr, and Pb isotope composition of the rocks in the Salmi batholith ($\varepsilon_{Nd}$ = -6.5 to -7.8; $\mu_2$ = 8.6 to 9.2; $\kappa_2$ = 4.1 to 4.5; $I_{Sr}$ = 0.7052 to 0.7057) indicate a single lower-crust source of a late Archean age.

Two alternative hypotheses concerning the generation of the magma for the Salmi batholith have been put forward.

1. The ascent of a mantle diapir up to the level of the lower crust resulted in partial melting of the lower crust. This made partial mixing of a secondary anatectic melt and the primary basaltoid one possible. However, due to the fundamental difference in concentrations of Pb, Nd, and Sr between the lower crust material and the mantle melt the isotope characteristics of these elements in the resulting melt remained the same as in the lower crust at the time of melting. Mixing calculations (Neymark et al., in prep.) suggest that the portion of the lower crust component in this mixed melt must be not less than 50 %. The subsequent differentiation of this melt resulted in generation of two complementary complexes, the gabbro-anorthosite-monzonite one and the rapakivi granite one. In the early stages of the evolution of the system it was possible that mantle material that was not contaminated by the secondary anatectic melt found its way to the upper crust and crystallized as basic dykes. According to Haapala and Rämö (1990) the diabase dykes in the northern exocontact area of the Wiborg batholith are of the same age as the rocks of the batholith but have somewhat different Nd isotopic composition ($\varepsilon_{Nd}$ values -1.0 to +1.6), which indicates that they were derived from the mantle and were not comagmatic with the Finnish rapakivi granites.
2. The ascent of a mantle diapir resulted in protrusion of considerable masses of basic magma at the base of the crust causing partial melting of the lower crust. Contamination of the primary basic magma by the material of the secondary anatectic magma may have led to a situation that the isotopic characteristics of Pb, Nd, and Sr in the contaminated magma became identical with those in the lower crust because of the marked differences in their concentrations in the lower crust and in the mantle. Crystallization of this magma may have resulted in the generation of the gabbro-anorthosite-monzonite complex. The latent heat released during the crystallization increases the partial melting of the material of the lower crust and caused generation of considerable volumes of a salic magma, the initial magma for the rapakivi granites.

The former hypothesis is more consistent with certain geochemical data.

## 9. RELATION OF THE MINERALIZATION IN THE PITKÄRANTA ORE DISTRICT TO THE SALMI BATHOLITH

Many questions regarding the genesis of the Pitkäranta deposits remain unsolved. Until now there exist a number of more or less justified viewpoints. As far as the relation of the mineralization to the hosting rocks is concerned, there are three main hypotheses:

syngenetic, epigenetic, and diplogenetic. The origin of the deposits have been explained as follows:

1. All mineralizations are genetically related to the rapakivi granites (Trüstedt, 1907; Hazov, 1973; Larin, 1980; Shergina et al., 1982).
2. All mineralizations are related to the later "activization granites" which are unrelated to the rapakivi and include the biotite and albite-protolithionite granites (Nikol'skaya & Gordienko, 1977).
3. Mineralization is of a polygenetic and polychronous nature. The iron-polymetallic ores are referred to as ancient stratiform deposits, syngenetic to the host rocks, while the tin and beryllium ores are considered epigenetic, genetically related to the rapakivi granites (Popov, 1975).
4. The mineralization is metamorphogenic, not related to the granitoids at all (Sudovikov, 1965).

At present most authors are of the opinion that the mineralizations in the Pitkäranta are genetically related to the granites of the Salmi batholith. In papers by Hazov (1973), Nikol'skaya and Gordienko (1977), Beljaev and Lvov (1981) the mineralogical and geochemical criteria for such an origin have been developed (see also Haapala, 1977). These include: 1) the geochemical specialization of the rapakivi granites and especially their later phases in elements like Be, Sn, W, Li, Cu, Zn, Pb, F, that constitute commercial-scale concentrations in the deposits; 2) the presence of accessory cassiterite, scheelite, beryl, sphalerite, chalcopyrite etc. in the late phase granites; 3) anomalously high contents of tin in the rock-forming minerals of the rapakivi granites, particularly in biotite (Hazov, 1973; Nikol'skaya & Gordienko, 1977).

Larin (1980) formulated the following criteria for the relationships of the Pitkäranta mineralizations to the granites of the Salmi batholith: 1) the affinity of the mineralization to the exocontact zone of the Salmi batholith (the zone of contact metamorphism) in the area of a fairly gentle plunge of the roof of the massif beneath the country rocks; 2) the one-way zonality of mineralization and metasomatosis in the scale of the entire ore district, going away from the Salmi batholith; 3) the sequential reduction of the role of the aposkarn greisens with beryllium, lithium and fluorite mineralization and the increase of the role of the aposkarn propylites with tin-polymetallic mineralization in proportion to the increasing depth of the albite-protolithionite granite domes; 4) a regular change of the concordant ore bodies into the intersecting and contact-following ones when going towards the Salmi batholith; 5) the identical character of the metasomatic zonality in the greisen-propylite bodies and the "around-the-veins" zonality around the dykes of albite-protolithionite granites in skarns.

An essential contribution to solving of the genetic problems of ore mineralization was made by the geochronological and isotope geochemical investigations of the magmatic rocks and ores in the region. These investigations resulted in verification of the statements on the similar age of the rocks of the Salmi batholith and that of the mineralization, as well as in establishing a common source for the ores and the magmatic rocks of the massif.

In conclusion it is worth emphasizing that the Salmi batholith, the only representative of the anorthosite - rapakivi granite assemblage in the Fennoscandian shield which contains a commercial ore mineralization, differs strictly from the other plutons in the following points: first, it is one of the youngest; secondly, its initial melt was generated by partial melting of the late Archean lower crust which was repeatedly reworked during the orogenic processes in the Proterozoic. The generation of the mineralization lasted more than 50 Ma and was affiliated to a single fluid-magmatic source of prolonged evolution. The stage I skarn ores were generated practically synchronously with the main (earliest) phase of the rapakivi granites while the stage II aposkarn ores were generated even after the crystallization of the final phases of the Salmi batholith but prior to the ultimate ending of the autometasomatic processes in the pluton. On the basis of the isotope characteristics of the ore lead and the common lead of the ore-bearing rapakivi granites, the Pitkäranta ore deposits can be classified as "deposits of rejuvenated cratons" (according to Zartman), which are regularly of a considerable size.

## DESCRIPTION OF THE EXCURSION ROUTES

All the excursion stops are marked on the route map (Fig. 27).

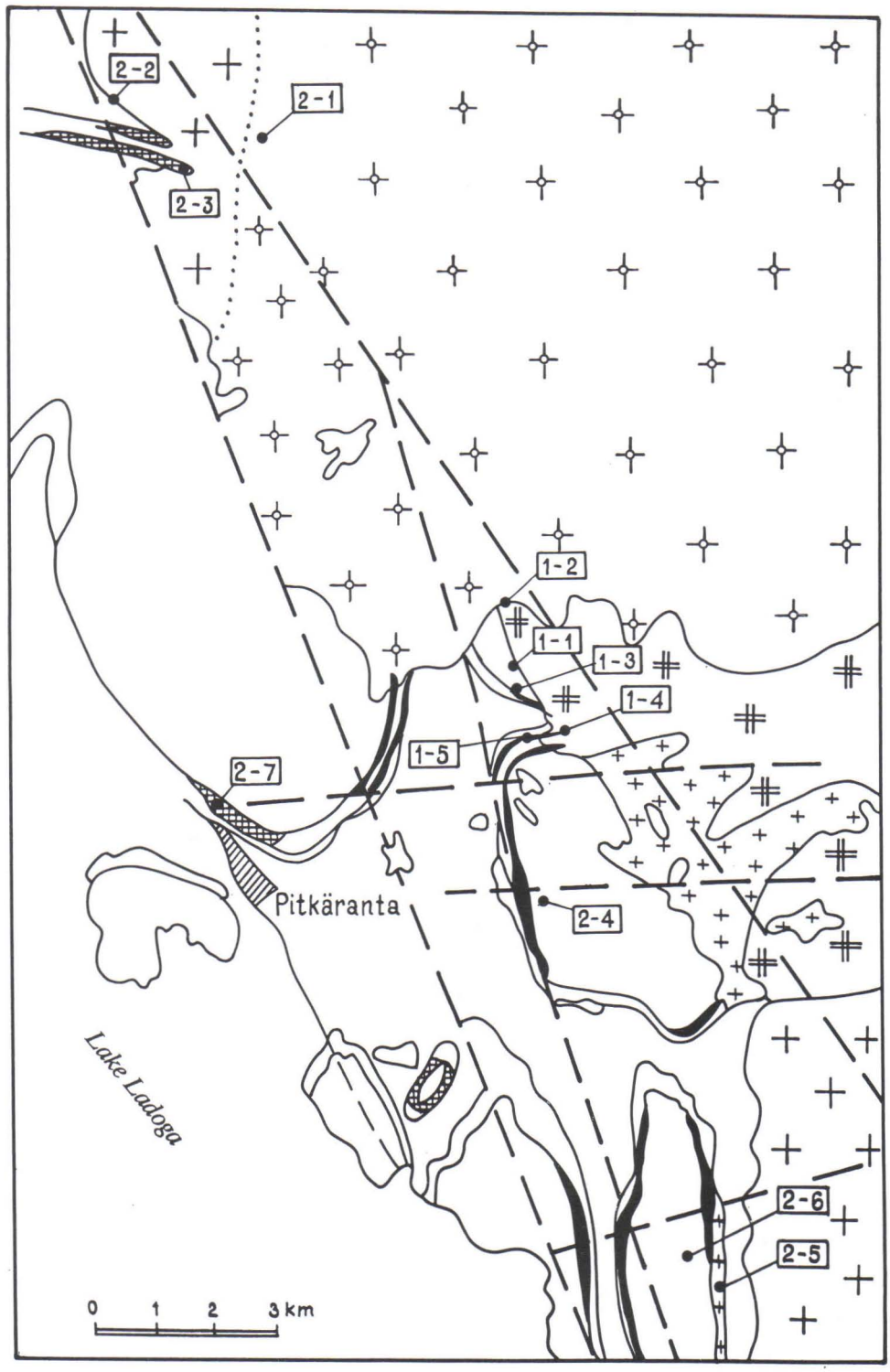


Fig. 27. Route map for the excursion. Stops are marked by number codes in rectangles; the codes include the day and the corresponding stop number.

## 1ST DAY. ROUTE: AREA OF THE HOPUNVAARA DEPOSIT - MUSTAVAARA HILL.

**Stop 1:** Porphyritic ovoidal amphibole-biotite granites (40 min).

A porphyritic ovoid-bearing amphibole-biotite granite with a fine-grained groundmass is exposed in a quarry. Potassium feldspar ovoids commonly up to 3 to 4 cm in diameter are surrounded by an oligoclase rim. In the western part of the outcrop the immediate contact between the porphyritic ovoid-bearing amphibole-biotite granite and the granite gneisses of the Vinberg dome is exhibited. The contact is sharp and the exocontact alterations poorly developed. In the 10 to 30 cm wide endocontact zone fine-grained granites occur; in composition they are close to the fine-grained groundmass of the porphyritic granites.

**Stop 2:** Contact of the biotite-amphibole and biotite granites (40 min).

500 m to the north from Stop 1 the immediate contact between the porphyritic amphibole-biotite granites with fine-grained groundmass and the even-grained biotite granites is seen. Fine-grained biotite granites occur in the endocontact zone of the biotite granites (20 to 50 cm in thickness). Exocontact alterations in the porphyritic amphibole-biotite granites are not present.

**Stop 3:** Greisenization zones with Be mineralization in the gneiss-granites of the Vinberg dome (20 min).

In the granite gneisses of the southern part of the Vinberg dome there occur zones of fluorite-phengite albitites, fluorite-albite-phengite and quartz-fluorite-phengite greisens carrying phenakite, bertrandite, and sometimes cassiterite.

**Stop 4:** Tract of the Klara I mine (1 h 20 min).

In the tract of the Klara I mine, in the northern part of the Lupikko granite gneiss dome, an exposed contact between the porphyritic amphibole-biotite granite and skarnized marbles of the upper carbonate horizon of the Pitkäranta suite occurs (Fig. 28). Albite-protolithionite granite dykes intersect the amphibole-biotite granites in an E-W direction parallel to the contact. In the dump areas magnetite-sphalerite-chalcopyrite

ore, skarnized, serpentinized, and fluoritized marble, and aposkarn greisen with beryllium mineralization are found (Figs. 14 and 15).

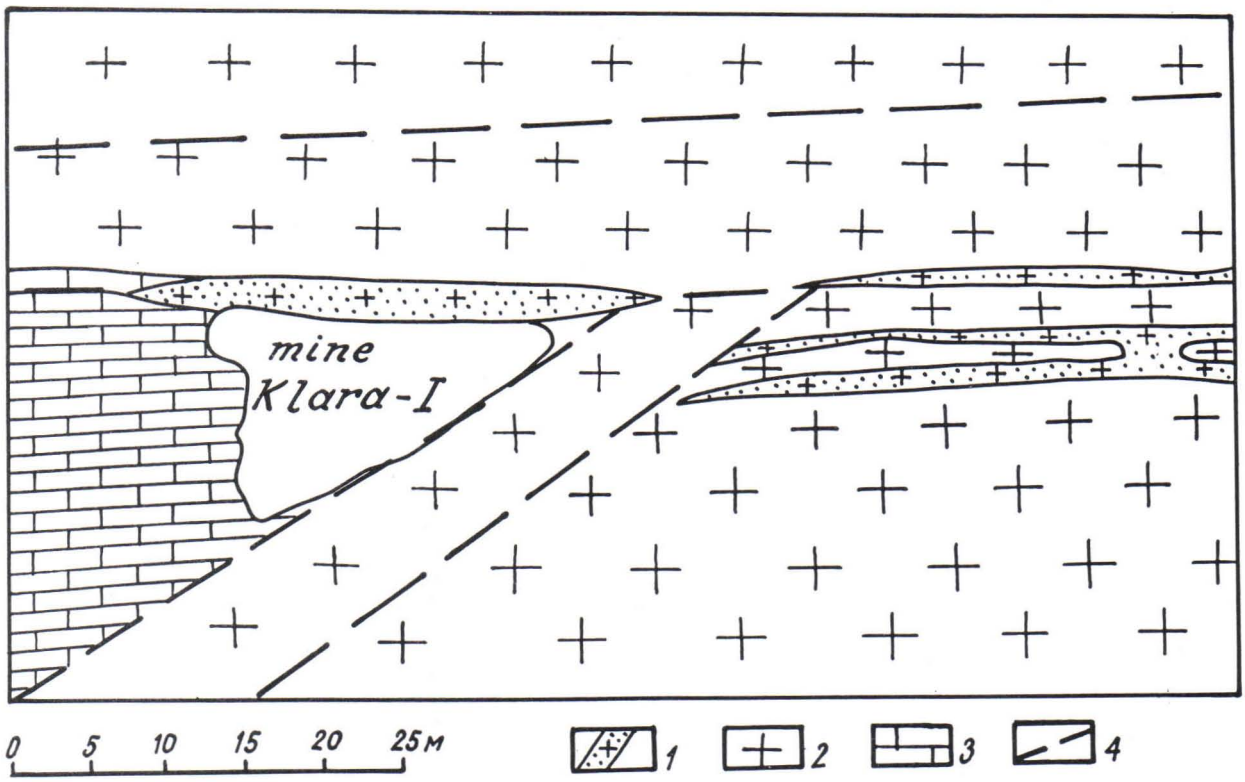


Fig. 28. Geology of the Klara mine. 1: dykes of fine-grained albite-protolithionite granites; 2: ovoidal anphibole-biotite granites; 3: marbles from the upper carbonate horizon in the Pitkäranta suite, from the framing of the northern part of the Lupikko granite gneiss dome; 4: cataclasis zones.

**Stop 5:** Magnetite quarry (1 h 20 min).

The magnetite quarry is situated in the northern part of the Lupikko granite gneiss dome within the rocks of the upper carbonate horizon of the Pitkäranta suite near the Hopunvaara deposit (Figs. 14 and 15). Between the mineralized marbles of the upper carbonate horizon and the biotite schists of the Ladoga series there is a 30 m thick, east striking synkinematic pegmatoid granite body. The northern contact of the granite with the biotite schists of the Ladoga series is sharp and winding. Minor boudined bodies of pegmatoid granite (diameter ca. 0.5 m) are found in the biotite schists. The southern contact of the pegmatoid granite body with the ore skarns is sharp and strikes east. The pegmatoid granite is intersected by thin (0.2-0.5 m) almost east-west-trending albite-protolithionite granite dykes.

Infiltration vein bodies of magnesian skarns and pipe-like, branching bodies of beryllium-bearing fluorite-vesuvianite-magnetite metasomatites occur in the dolomite marbles of the upper horizon. The latter are characterized by concentrically-zoned frilly structures.

## 2ND DAY. ROUTE: REPOMÄKI - KITELÄ DEPOSIT - LUPIKKO - UUKSU.

**Stop 1:** Porphyritic biotite granite (30 min).

In a quarry on the Repomäki hill there is an exposure of porphyritic biotite granite with a fine-grained groundmass. The granites are intersected by dykes of fine-grained biotite granites. The biotite granites are slightly albitized and muskovitized. Their Li, Rb, Nd, Sn, Be, U, and Th contents are higher than those in the unaltered biotite granites (Fig. 5).

**Stop 2:** Tract of Kitelä mine. Contact of biotite granites and schists of the Ladoga series (20 min).

Exposed at this site is a winding contact between the biotite granites and the schists of the Ladoga series. Granites plunge below the rocks of the Ladoga series. In the biotite schists there is an intersecting vein of fine-grained biotite granite, striking north. Exocontact alterations in the biotite schists are scarse. Endocontact alterations in the granites have resulted in an enrichment of quartz (black bipyramidal crystals). The thickness of the endocontact zone is 0.5 m.

**Stop 3:** Kitelä mine (40 min).

The deposit is situated in the northern part of the Pitkäranta ore district at the contact of the Salmi batholith (Figs. 29-30). The ore bodies are associated with the lower and, to a lesser extent the upper carbonate horizons of the Pitkäranta suite enclosing the granite gneisses of the Pitkäranta-Koirinoja dome. In the eastern part of the deposit the ore bodies build up inlets projecting into the even-grained biotite granites. The rapakivi granites plunge steeply to the west. The thickness of the ore bodies varies from 4 to 30 m and the length is several hundred meters. The magnetite-sphalerite and tin mineralization is associated with lime skarns and skarn-neighboring rocks of the first

stage of ore generation. The tin-polymetallic mineralization is associated predominantly with actinolite aposkarn propylites and less commonly with feldspar metasomatites of the second stage of ore generation.

The Kitelä deposit is the main tin lode in the region.

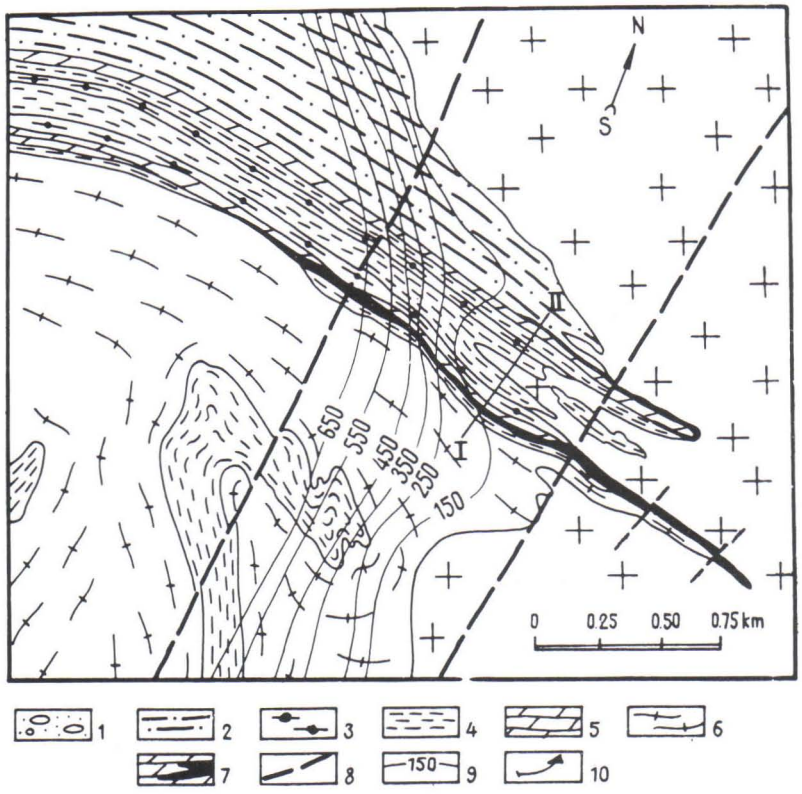


Fig. 29. Geological structure of the Kitelä mine. 1: Quarternary deposits; 2: schists of the Ladoga series; 3-5: Pitkäranta suite: 3 - graphite schists, 4 - amphibole schists and amphibolites, 5 - carbonate horizons; 6: granite gneiss; 7: ore bodies; 8: fractures; 9: depth of the roof of the Salmi batholith beneath the overlying rocks; 10: drill holes.

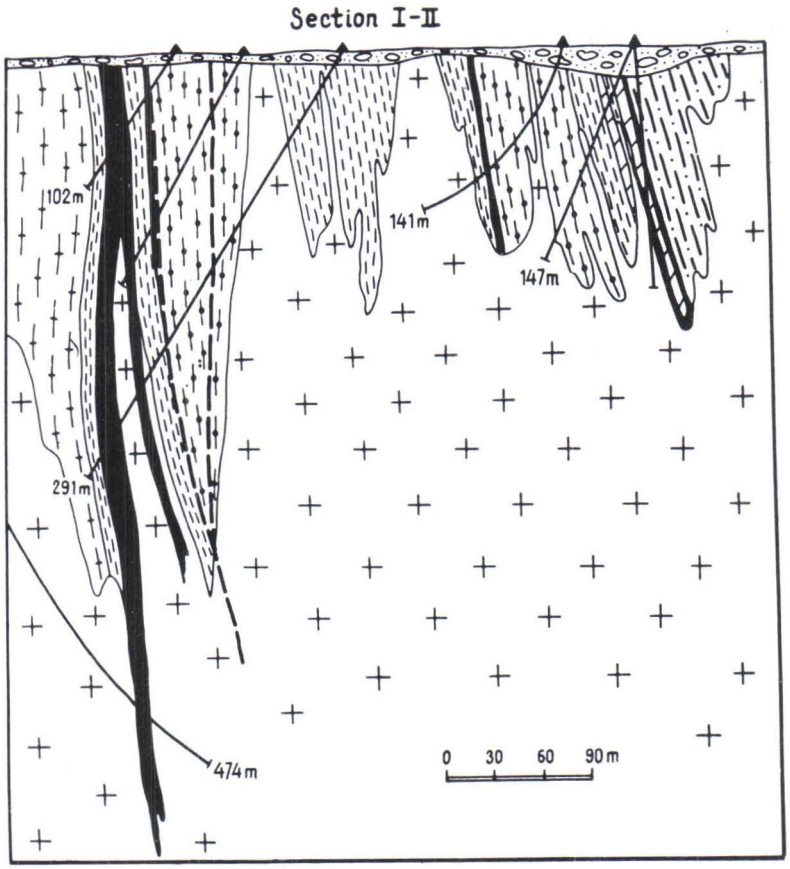


Fig. 30. Cross-section along the profile I-II. Kitelä deposit. Legend the same as in Fig. 29.

**Stop 4:** The Lupikko quarries, pegmatites, and granite porphyries (1 h).

The site is in the western part of the Lupikko granite gneiss dome. Large bodies of late-kinematic ceramic pegmatites are located at the contact between granite gneisses and the rocks of the Pitkäranta suite. A series of granite porphyry and quartz porphyry dykes,showing northwest-trending en echelon structures occur in the granite gneisses. Thickness of the dykes is very variable with a maximum of 30 m. According to discrimination analysis of petrochemical data, the granite porphyries correspond to the porphyritic amphibole-biotite rapakivi granites. As shown in Fig. 31, the granite porphyry dykes contain numerous xenoliths of granite-gneiss, amphibolite, garnet-diopside skarn, biotite schist of the Ladoga series, pegmatite and amphibole-biotite granites (both even-grained and porphyritic). High concentrations of tin are observed in some xenoliths of garnet-diopside skarn (up to 0.3 %) and in xenoliths of microclinized amphibolite (up to 42 g/tn). The concentration of tin in the granite porphyry is 3.5-4

g/tn. The granite porphyry is intersected by albite-protolithionite granite dykes which are 10 to 25 cm thick and trend northeast; minor xenoliths of granite porphyry also occur. The tin content of the albite-protolithionite granite is 4.5-5.7 g/tn.

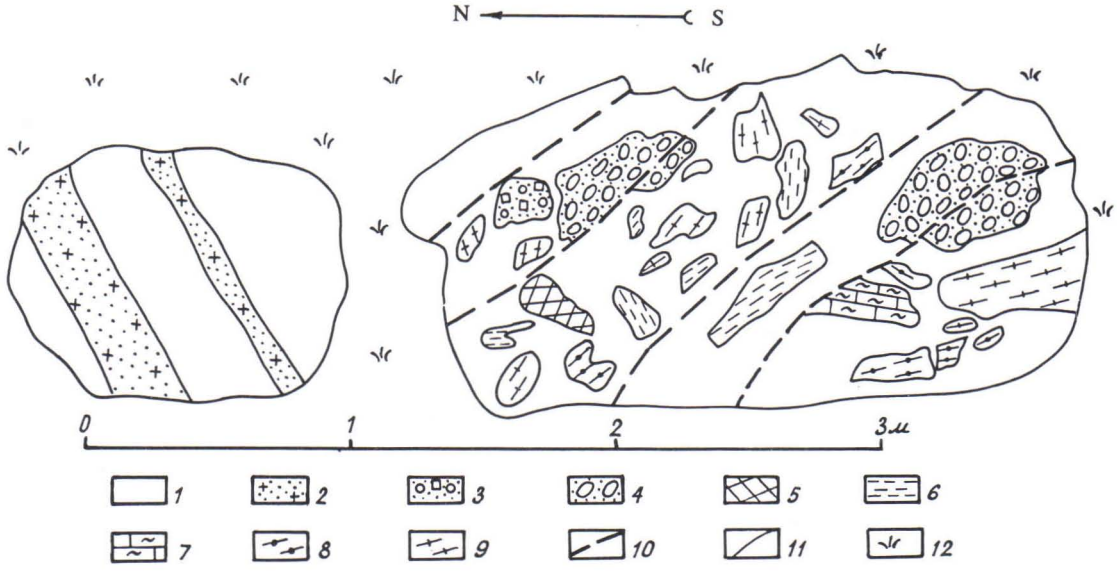


Fig. 31. Map of an outcrop of a granite porphyry dyke in the granite gneisses of the Lupikko dome. In the right part of the outcrop a magmatic granite porphyry breccia is met with and in the left part veins of fine-grained albite-protolithionite granites that cut the granite porphyries occur. 1: granite porphyry; 2: albite-protolithionite granite; 3-9: xenoliths: 3 - porphyritic amphibole-biotite granite with a fine-grained groundmass, 4 - ovoidal porphyritic amphibole-biotite granite with a fine-grained groundmass, 5 - ceramic pegmatites, 6 - biotite schists, 7 - skarnized marbles, 8 - microclinized amphibolites, 9 - granite-gneiss; 10: cracks; 11: boundaries of the outcrop; 12: soil.

**Stop 5:** Albite-protolithionite granites around the Uuksu village (1 h).

The albite-protolithionite granites intersect the granite-gneisses of the Uuksu dome structure forming gently plunging 0.2 to 0.8 m thick dykes. The central parts of these dykes consist of a fine-grained albite-protolithionite granite and the 10 to 20 cm thick marginal parts of pegmatoid materials (stockscheiders).

In the largest, gently plunging albite-protolithionite granite body in the endocontact zone rhythmical banding is present in the fine-grained albite-protolithionite granite. Immediately in the endocontact zone large (5 to 10 cm) skeletal quartz crystals and potassium feldspar porphyroblasts intersect the banding. Large topaz crystals are found also (Fig. 3).

Geochemical profiles across the contact between the albite-protolithionite granites and the hosting granite gneisses show that in the endocontact zone there is a strong increase in the contents of Sn, Be, Li, and Rb, while no changes in the content of these elements occur in the exocontact zone.

**Stop 6:** Drill core inspection, Uuksu village (1 h).

1. Contact between a stock of albite-protolithionite granite and a biotite schist of the Ladoga series.
2. Quartz monzonite from the southern part of the Salmi batholith.
3. Tin-polymetallic ore body, Kitelä deposit (aposkarn propylites and garnet skarns).
4. Beryllium-tin ore body, Uuksu deposit (aposkarn greisens).
5. Jotnian terrigenous-volcanogenous complex (Salmi suite).
6. Dolerites, monzonites, and monzodiorites from the Jotnian Hopunvaara intrusion that intersects the rapakivi granites and mineralized skarns.

**Stop 7:** Mines of the Old Ore Field, Pitkäranta town (40 min).

The Old Ore Field is situated in the central part of the ore district in the south-western frame of the Pitkäranta-Koirinoja dome, some three km west from the Salmi batholith. According to geophysical data the roof of the batholith lies here at a depth of at least one km. The ore deposits follow predominantly the lower carbonate horizon. As far as the character of the mineralization and the ore-bearing metasomatic rocks is concerned, the deposits of the Old Ore Field are very similar to the Kitelä deposit.

## References

**Amelin, Yu.V., Neymark, L.A., Larin, A.M. et al., 1990. Амелин, Ю.В., Неймарк, Л.А., Ларин, А.М. и дп., 1990.** Возраст руд Питкярантского рудного района (Северное Приладожье) и их связь с гранитами рапакиви Салминского массива (Age of the ores of the Pitkäranta ore district, Northern Ladoga Region, and their relation to the rapakivi of the Salmi massif). В кн.: Изотопное датирование эндогенных рудных формаций. Тез. докл. всесоюзного совещания, Киев, 155-157 (Апатиты).

**Anderson, J.L., 1983.** Proterozoic anorogenic granite plutonism of the North America. *In* L.G. Medaris, C.W. Byers, D.M. Mickelson and W.C. Shanks (Editors), Proterozoic Geology: selected papers from an international Proterozoic Symposium. Geological Society of America Memoir, 161, 133-154.

**Bantova, M.A., Levkovskiy, R.Z. & Sharkov, V.E., 1975. Бантова, М.А., Левковский, Р.З. & Шарков, В.Е., 1975.** Геология, вещественный состав и возраст пород Салминского комплекса гранитов рапакиви и габбро-анортозитов (Geology, composition and age of the rocks of the Salmi rapakivi granite and gabbro-anorthosite complex). Сов. геология, 7, 78-86.

**Barker, D., Wones, D.R., Sharp, W.N. & Desborough, G.A., 1975.** The Pikes Peak batholith, Colorado Front Range, and a model for the origin of the gabbro-anorthosite-syenite-potassic granite suite. Precambrian Research, 2, 97-160.

**Beljaev, A.M., 1985. Беляев, А.М., 1985.** Закономерности распределения рудных элементов в пегматоидных гранитах и гранито-гнейсах Северного Приладожья (Regularities in the distribution of the ore-forming elements in the pegmatoid granites and granite gneisses of the Northern Ladoga Region). В кн.: Закономерности концентрации рудных элементов в гранитоидных формациях Карело-Кольского региона, 89-96 (Апатиты)

**Beljaev, A.M., 1987. Беляев, А.М., 1987.** Геохимическая характеристика пород приконтактовых зон гранитов рапакиви Салминского массива (Geochemical characteristics of the rocks of the contact zones in the rapakivi granites of the Salmi massif). Вестник ЛГУ, вып. 3(21), 80-83.

**Beljaev, A.M. & Lvov, B.K., 1981. Беляев, А.М. & Львов, Б.К., 1981.** Минералого-геохимическая специализация гранитов рапакиви Салминского массива (Mineralogical-geochemical specialization of the rapakivi granites of the Salmi massif). Вестник ЛГУ, 6, 15-24.

**Birks, A.P. & Koshik, L.I., 1984. Биркс, А.П.& Кошик, Л.И., 1984.** Анортозиты поздних этапов развития Восточно-Европейской платформы (Anorthosites of the late stages in the development of the Eastern European platform). В кн.: Анортозиты Земли и Луны. Труды ГИН АН СССР, вып. 375. Наука, 272 с.

**Bogatikov, O.A., Sharkov, E.V. & Suhanov, M.K., 1985. Богатиков, О.А., Шарков, Е.В. & Суханов, М.К., 1985.** Анортозиты докембрия (Anorthosites of the Precambrian). Магматические горные породы, 3. Наука, Моцква, 240-277.

**Bridgwater, D. & Windley, B.F., 1973.** Anorthosites, post-orogenic granites, acid volcanic rocks and crustal development in the North Atlantic Shield during the mid-Proterozoic. *In* Symposium on granites, gneisses and related rocks. Special Publications of Geological Society of Africa, 3, 307-318.

**Daoud, W.K. & Fuck, R.A., 1989.** Tin-bearing granites of Petinga mine, Amazonas, Brasil: geological context and associated ore deposits. *In* Symposium Precambrian granitoids, Abstracts. Geological Survey of Finland Special Paper, 8, 35.

**Emslie, R.F., 1985.** Proterozoic anorthosite massifs. *In* A.C. Tobi and J.L.R. Touret (Editors), The deep Proterozoic crust in the North Atlantic Provinces, 39-60.

**Eskola, P., 1951.** Around Pitkäranta. Annales Academiæ Scientiarum Fennicæ, A III 27, 90 p.

**Foster, M.D., 1960.** Interpretation of the composition of lithium micas. U.S. Geological Survey Professional Paper, 354-E.

**Fountain, J.C., Hodge, D. & Hills, F.A., 1981.** Geochemistry and petrogenesis of the Laramic Anorthosite Complex. Lithos 14, 113-132.

**Furman, G., 1812. Фурман, Г., 1812.** Минералогические замечания, собранные в Старой финляндии в Сердобольском и Новой финляндии в Куопиевском уездах (Mineralogical observations collected in the Serdobol district, Old Finland, and in Kuopio district, New Finland). Технологический журнал, IX, 4.

**Haapala, I., 1977.** The controls of tin and related mineralization in the rapakivi areas in south-eastern Fennoscandia. Geologiska Föreningens i Stockholm Förhandlingar, 99, 130-142.

**Haapala, I. & Rämö, O.T., 1990.** Petrogenesis of the Proterozoic rapakivi granites of Finland. *In* H.J. Stein and J.L. Hannah (Editors), Ore-bearing granite systems; Petrogenesis and mineralizing processes. Geological Society of America Special Paper, 246, 275-286.

**Hazov, R.A., 1967. Хазов, Р.А., 1967.** Новое проявление оловянного оруденения в Северном Приладожье (Кительское месторождение) (A new occurence of tin mineralization in the Northern Ladoga Region -the Kitelä deposit). Сов. геология, 7, 119-125.

**Hazov, R.A., 1973. Хазов, Р.А., 1973.** Геологические особенности оловянного оруденения Северного Приладожья (Geological characteristics of the tin mineralization in the Northern Ladoga Region). Наука, Ленинград, 87 с.

**Higgins, M.D. & Doig, R., 1981.** The Sept Iles anorthosite complex: field relationships, geochronology and petrology. Canadian Journal of Earth and Science, 18(3), 561-573.

**Kleeman, G.J & Twist, D., 1989.** Composition-zoned Sheet-like Granite Pluton of Bushveld Complex: Evidence Bearing on the Nature of A-type magmatism. Journal of Petrology, 30(6), 1383-1414.

**Kolker, A., Lindsley, D.H. & Hanson, G.N., 1990.** Geochemical evolution of the Maloin Ranch pluton, Laramie anorthosite complex, Wyoming: Trace elements and petrogenetic models. American Mineralogist, 75, 572-588.

**Kranck, E.H., 1968.** Anorthosites and rapakivi, magmas from the lower crust. *In* Y.W. Isachsen (Editor), Origin of anorthosite and related rocks. New York State Museum and Science Service Memoir, 18, 93-97.

**Larin, A.M., 1980. Ларин, А.М., 1980.** Особенности проявления зональности минерализации в Питкярантском рудном районе (Peculiarities in the zonality of the mineralization in the Pitkäranta ore district) Бюлл. МОИП, отд. геол., 55, вып. 3, 73-82.

**Larin, A.M., Neymark, L.A., Gorohovskiy, B.M. and Ovchinnikova, G.V., 1990. Ларин, А.М., Неймарк, Л.А., Гороховский, Б.М., Овчинникова, Г.В., 1990.** Связь комплексного скарнового оруденения Питкярантского района с гранитами рапакиви Салминского массива по Pb-изотопным данным (Connection of the complex skarn mineralization of the Pitkäranta district with the rapakivi granites of the Salmi massif according to Pb isotope data). Известия АН СССР, сер. геол., 5, 47-57.

**Levkovskiy, R.Z., 1975. Левковский, Р.З., 1975. Рапакиви** (Rapakivi). Наука, Ленинград, 224 с.

**Liew, T.C. and Hofmann, A.W., 1988.** Precambrian crustal components, plutonic associations, plate environment of the Hercynian Fold Belt of Central Europe: Indications from Nd and Sr isotopic study. Contributions to Mineralogy and Petrology, 98(2), 129-138.

**Ludwig, K.R., 1988.** ISOPLOT - a plotting and regression program for radiogenic-isotope data, for IBM-PC compatible computers, version 2. U.S. Geological Survey Open File Report, 88-557.

**Lundqvist, T., 1979.** The Precambrian of Sweden. Sveriges Geologiska Undersökning, Serie C, NR 768, Upsala, 65 p.

**Nikol'skaja, J.D. & Gordienko, L.I., 1977. Никольская, Ж.Д. & Гордиенко, Л.И., 1977.** Петрология и металлогения гранитоидных формаций Карелии (Petrology and metallogeny of the granitoid assemblages of Karelia). Недра, Ленинград, 152 с.

**Nurmi, P.A. & Haapala, I., 1986.** The Proterozoic Granitoids of Finland: Granite types, metallogeny and relation to crustal evolution. Bulletin of the Geological Society of Finland, 58, Part 1, 203-233.

**Palmunen, M.K., 1939.** Pitkäranta vv. 1934-1938 suoritettujen vuoriteknillisten tutkimusten valossa. Geologinen toimikunta, Geoteknillisiä julkaisuja, 44, 154 p.

**Patchett, P.J., 1978.** Rb-Sr ages of precambrian dolerites and syenites in Southern and Central Sweden. Sveriges Geologiska Undersökning, Serie C, NR 747, Upsala, 65 p.

**Pearce, J.A., Harris, N.B.W. and Tindle, A.G., 1984.** Trace element discrimination diagrams for the tectonic interpretation of granitic rocks. Journal of Petrology, 25, 956-983.

**Popov, V.E., 1975. Попов, В.Е., 1975.** О новом типе местопождений областей тектоно-магматической активизации (на примере юга Карелии и других регионов) (On a new mineral deposit type in the regions of tectono-magmatic activization), В кн.: Закономерности размещения полезных ископаемых, XI, Наука, Москва, 235-243.

**Rämö, O.T. & Haapala, I., 1991.** The rapakivi granites of eastern Fennoscandia: a review with insights into their origin in the light of new Sm-Nd isotopic data. *In* C.F. Gower, T. Rivers & B. Ryan (Editors), Mid-Proterozoic Laurentia-Baltica. Geological Association of Canada Special Paper, 38, in print.

**Rämö, O.T., Huhma, H. & Vaasjoki, M., 1990.** Protolith variation in the Proterozoic rapakivi granites of eastern Fennoscandia: Nd and Pb isotopes. 7th International Conference on Geochronology, Cosmochronology and Isotope Geology Abstract Volume, Geological Society of Australia Abstracts, 27, 81.

**Scherbak, N.P. et al., 1989. Щербак, Н.П. и др., 1989.** Геохронологическая шкала докембрия Украинского щита. Киев, 144 с.

**Sharkov, E.V., 1974. Шарков, Е.В., 1974.** Массивы метагаббро-лабрадоритов - мангеритов Колвицких, Кандалакшских и Сальных тундр (Кольский полуостров) как интрузии шовного типа зоны глубинного разлома (Massifs of metagabbro-labradorite to mangerite in the Kolvitsa, Kandalaksha and Sal'nye Hills, Kola peninsula - intrusions of suture type in a deep fracture zone). Анортозиты СССР. Москва, 30-41.

**Shergina, JU.P., Larin, A.M., Chuhonin, A.P. et al., 1982. Шергина, Ю.П., Ларин, А.М., Чухонин, А.П. и др., 1982.** Возраст Салминского массива гранитов рапакиви и связанного с ним оруденения (Age of the Salmi rapakivi granite massif and the related mineralization). Известия АН СССР, сер. геол., 12, 64-76.

**Shinkarev, N.F. & Anischenkova, O.N., 1973. Шинкарев, Н.Ф. & Анищенкова, О.Н., 1973.** Новые данные о составе и строении Салминского комплекса рапакиви (New data on the composition and structure of the Salmi rapakivi complex). Известия АН СССР, сер. геол., 2, 140-144.

**Shinkarev, N.F. & Ivannikov, V.V., 1983. Шинкарев, Н.Ф. & Иванников, В.В., 1983.** Физико-химическая петрология изверженных пород (Physico-chemical petrology of igneous rocks). Недра, Ленинград, 271 с.

**Shinkarev, N.F., Ivannikov, V.V., Lapshin S.G. & Leonova V.A., 1987. Шинкарев, Н.Ф., Иванников, В.В., Лапшин С.Г. & Леонова В.А., 1987.** Геохимические критерии происхождения докембрийских гранитов в свете идей В.И. Вернадского (на примере Балтийского щита) В кн.: Геохимические идеи В.И. Вернадского в наши дни. ЛГУ, Ленинград, 54-74.

**Simonen, A., 1980.** The Precambrian in Finland. Geological Survey of Finland Bulletin, 304, 58 p.

**Stacey, J.S. & Kramers, J.D., 1975.** Approximation of terrestrial lead isotope evolution by two-stage model. Earth and Planetary Science Letters, 26, 207-221.

**Sudovikov, N.G., 1965. Судовиков, Н.Г., 1965.** Метаморфогенное рудообразование (Metamorphogene ore mineralization). Сов. геология, 1, 105-119.

**Sviridenko, L.P., 1968. Свириденко, Л.П., 1968.** Петрология Салминского массива гранитов рапакиви (в Карелии) (Petrology of the Salmi rapakivi granite massif, Karelia). Петрозаводск, 116 с.

**Sviridenko, L.P., Svetov, A.P., Golubev, A.I. & Pavlov, G.M., 1984. Свириденко, Л.П., Светов, А.П., Голубев, А.И. & Павлов, Г.М., 1984.** Топазсодержащие туффизиты южной окраины Балтийского щита (Topaz bearing tuffisites of the southern boundary of the Baltic shield). Докл. АН СССР 276(6), 1449-1452.

**Taylor, S.R. & McLennan, S.M., 1985.** The continental crust: its composition and evolution. Blackwells, Oxford, 312 p.

**Trüstedt, O., 1907.** Die Erzlagerstätte von Pitkäranta am Ladoga-See. Bulletin de la Commission Géologique de Finlande, 19.

**Törnebohm, A.E., 1891.** Om Pitkäranta malmfält och dess omgifningar. Geologiska Föreningens i Stockholm Förhandlingar, Bd. XIII, 313-334.

**Vaasjoki, M., 1977.** Rapakivi granites and the other postorogenic rocks in Finland: their age and the lead isotopic composition of certain associated galena mineralizations. Geological Survey of Finland Bulletin, 294, 66 p.

**Vaasjoki, M., Rämö, O.T. & Sakko, M., 1991.** New U-Pb ages from Wiborg rapakivi area: constraints on the temporal evolution of the rapakivi granite - anorthosite - diabase dyke association of Southeastern Finland. Precambrian Research, 51 (in print).

**Velikoslavinskiy, D.A. et al. (15 authors), 1978. Великославинский, Д.А. и др. (15 авторов), 1978.** Анортозит-рапакивигранитная формация Восточно-Европейской платформы (Anorthosite - rapakivi granite assemblage of the Eastern European platform). Наука, Ленинград, 296 с.

**Vinogradov, A.P., 1962. Виноградов, А.П., 1962.** Средние содержания химических элементов в главных типах изверженных горных пород земной коры (Average contents of chemical elements in the main types of the igneous rocks in the Earth crust). Геохимия, 7, 555-571.

**Vorma, A., 1976.** On the petrochemistry of rapakivi granites with special reference to the Laitila massif, southwestern Finland. Geological Survey of Finland Bulletin, 285, 95 p.

**Welin, E. & Lundqvist, T., 1975.** K-Ar ages of Jothnian dolerites in Västernorrland County, Central Sweden. Geologiska Föreningens i Stockholm Förhandlingar, 97, 83-87.

**Welin, E. & Lundqvist, T., 1984.** Isotopic investigations of Nordingrå rapakivi massif, north-central Sweden. Geologiska Föreningens i Stockholm Förhandlingar, 106, Pt. 1, 41-49.

**Welin, E., Vaasjoki, M. & Suominen, V., 1983.** Age differences between Rb-Sr whole rock and U-Pb zircon ages of syn- and postorogenic Svecokarelian granitoids in Sottunga, SW Finland. Lithos, 16, 297-305.

**Windley, B.F., 1983.** A tectonic review of Proterozoic. *In* L.G. Medaris, C.W. Byers, D.M. Mickelson and W.C. Shanks (Editors) Proterozoic Geology, Selected Papers from an international Proterozoic Symposium, Geological Society of America Memoir, 161, 1-10.

Tätä julkaisua myy

GEOLOGIAN
TUTKIMUSKESKUS (GTK)
Julkaisumyynti
02150 Espoo
☎ (90) 46931
Teleksi 123185 geolo sf
Telekopio (90) 462205

GTK. Väli-Suomen
aluetoimisto
Kirjasto
PL 1237
70701 Kuopio
☎ (971) 205111
Telekopio (971) 205215

GTK. Pohjois-Suomen
aluetoimisto
Kirjasto
PL 77
96101 Rovaniemi
☎ (960) 279219
Teleksi 37295 geolo sf
Telekopio (960) 297289

Denna publikation säljes av

GEOLOGISKA
FORSKNINGSCENTRALEN (GFC)
Publikationsförsäljning
02150 Esbo
☎ (90) 46931
Telex 123185 geolo sf
Telefax (90) 462205

GFC. Distriktsbyrån för
Mellersta Finlands
Biblioteket
PB 1237
70701 Kuopio
☎ (971) 205111
Telefax (971) 205215

GFC. Distriktsbyrån för
Norra Finlands
Biblioteket
PB 77
96101 Rovaniemi
☎ (960) 297219
Telex 37295 geolo sf
Telefax (960) 297289

This publication can be obtained
from
GEOLOGICAL SURVEY
OF FINLAND (GSF)
Publication sales
SF-02150 Espoo, Finland
☎ +358 0 46931
Telex 123185 geolo sf
Telefax +358 0 462205

GSF. Regional office for
Mid-Finland
Library
P.O.Box 1237
SF-70701 Kuopio, Finland
☎ +358 71 205 111
Telefax +358 71 205 215

GSF. Regional office for
Northern Finland
Library
P.O.Box 77
SF-96101 Rovaniemi, Finland
☎ +358 60 297 219
Telex +358 60 37 295 geolo sf
Telefax +358 60 297 289

GEOLOGICAL SURVEY OF FINLAND, Opas — Guide 33, Ilmari Haapala, O. Tapani Rämö, and Pekka T. Salonsaari (Editors)

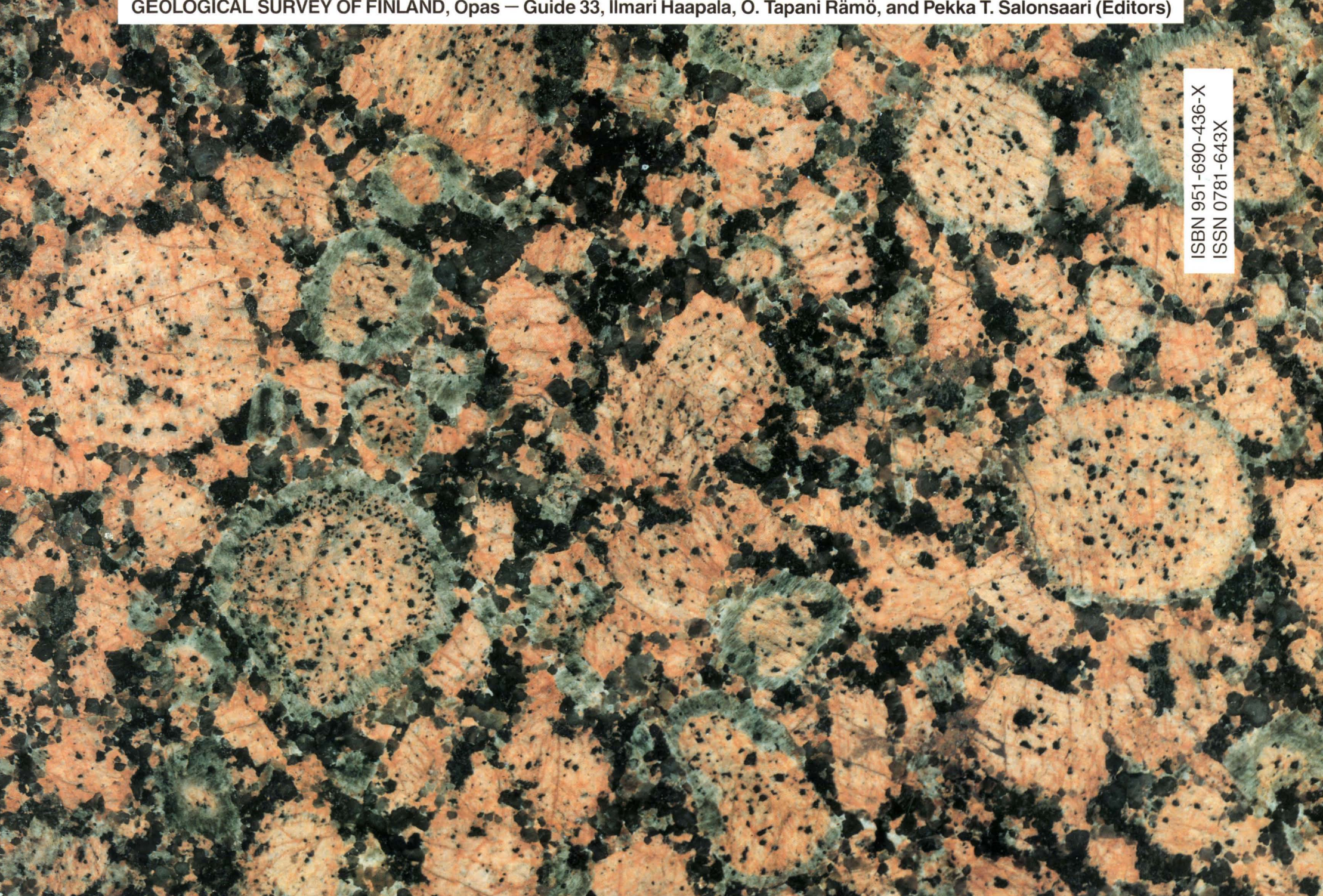

ISBN 951-690-436-X
ISSN 0781-643X